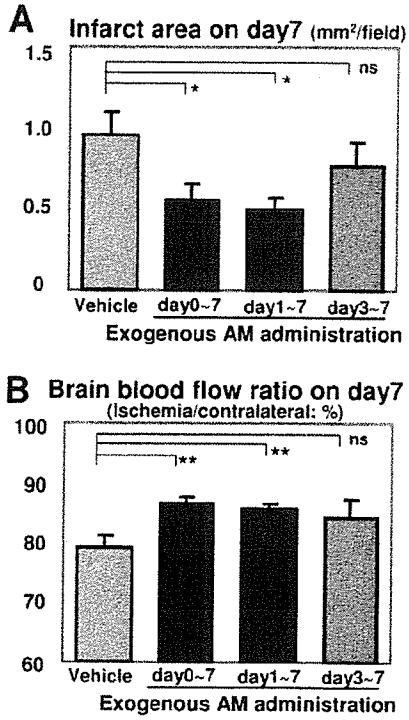


FIG. 9. Effects of exogenously administrated AM on neuroprotection and vascular regeneration after 20m-MCAO. 50 ng/h AM was administrated to mice with an ip implanted osmotic pump. Infarct area (A) and blood flow (B) on postoperative d 7 with different starting points for AM administration. *, $P < 0.05$; **, $P < 0.01$; ns, not significant *vs.* vehicle; n = 6.

lature, the so-called "vascular niche" (35), where endothelial cells secrete neurogenic factors, including basic fibroblast growth factor, vascular endothelial growth factor, and brain-derived neurotrophic factor, and create conditions conducive to neurogenesis (36). Therefore, vascular regeneration is assumed to rescue ischemic brain via not only supply of oxygen and nutrition but also promotion of neurogenesis. We confirmed in this study that neurogenesis occurred adjacent to neovessels in the ischemic core and the number of regenerated neurons was correlated with vascular density.

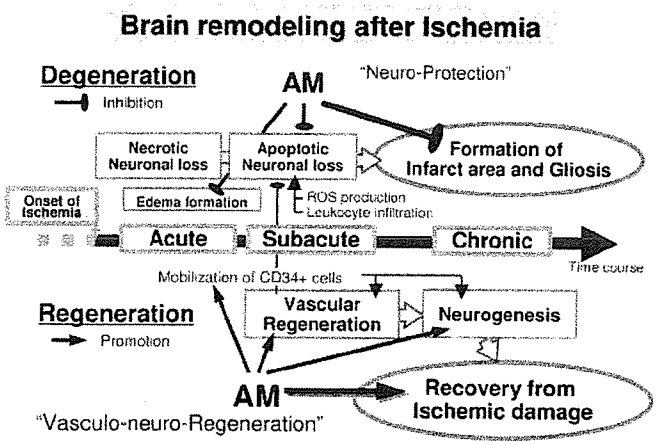


FIG. 10. Summary of brain remodeling after ischemia and effects of AM on the ischemic brain observed in this study.

We have assigned the term "vasculo-neuro-regeneration" to the entire process of enhancement of vasculogenesis and subsequent neurogenesis.

We demonstrated that AM promotes vasculo-neuro-regeneration in the ischemic brain. Blood flow and capillary density in the ischemic brain after 20m-MCAO was significantly enhanced in AM-Tg mice after postoperative d 7 with subsequent promotion of neurogenesis after d 28. The promoted vasculogenesis and neurogenesis observed in AM-Tg mice was significantly correlated with the functional recovery after 20m-MCAO. This result suggests that these two regenerative elements might contribute to the functional recovery after 20m-MCAO. The neovascularization was preceded by augmented mobilization of $CD34^+$ mononuclear cells, which are known to differentiate into endothelial cells and contribute to vasculogenesis (37). Recently, iv infusion of $CD34^+$ cells has reported to promote not only neovascularization but also neurogenesis (38). Furthermore, we observed the direct promoting action of AM on neural differentiation of PC12 cells via cAMP/PKA- and PI3K/Akt-dependent pathways. The totality of these findings suggests that the neurogenic action of AM *in vivo* comprises at least two different mechanisms: a direct action on neuronal cells through activation of PKA and Akt and an indirect action on neurogenesis after enhanced neovascularization.

Judging from the ratio of mature AM to total AM as shown in Table 1, the mature AM concentration in the ischemic brain of AM-Tg mice was expected to be 1~4 fmol/g tissue. The concentration seems to be comparable to the reported effective concentration of mature AM *in vivo* (25, 39). The *in vivo* concentration of human mature AM in the whole brain (1 fmol/g tissue level) and in the plasma (10 fmol/ml level) might be lower than the minimal concentration required for its *in vitro* action (100 fmol/ml) observed in this study. The actual effective concentration *in vitro*, however, might be lower because the administrated peptide is rapidly degradated *in vitro*. In addition, it is demonstrated in previous reports including ours (40, 41), that peptides could exert their significant actions at the stably maintained concentration, that is, by 2 orders of magnitude lower than that of bolus administration. In AM-Tg mice, the AM concentration was maintained at the same level due to the constitutive overproduction by the human serum amyloid P component promoter. Thus, we suppose that the direct neuronal action of AM *in vivo* could be possible in this stroke model.

In view of clinical application, we also tried exogenous administration of AM by ip implanted osmotic pump to determine appropriate amount and timing of AM administration after 20m-MCAO. Previous reports on AM administration for rodents or human set the therapeutic dose at 2~25 fmol/ml (25, 39). For our experiments, therefore, we used two lines of transgenic mice with a plasma concentration of mature AM of 24.9 ± 4.2 and 2.6 ± 0.6 fmol/ml. The results showed comparable effects of AM in these two lines on neuroprotection and vascular regeneration. This led us to conclude that a plasma level of 2~3 fmol/ml of mature AM, 3~5 times higher than its physiological concentration, was sufficient to attain therapeutic effects for the mice after 20m-MCAO. We next tried exogenous infusion of AM with an osmotic pump in the amount reported to achieve a plasma

concentration of 2~3 fmol/ml. The exogenous AM treatment which started just after the induction of 20m-MCAO or at 24 h after produced significant effects that were comparable to those seen in the two lines of AM-Tg mice. However, that from 72 h postoperatively failed to reveal significant effects. These results showed that appropriate timing to start AM administration after stroke is less than 72 h after the event.

We performed two different stroke models, nonfatal 20m-MCAO and fatal 2 h-MCAO. In 2 h-MCAO, we observed significant reduction of brain edema in AM-Tg mice through reduction of vascular permeability, which is compatible with previous report (42). However, infarct size was not reduced on postoperative d 1 after 2 h-MCAO. The result suggests that AM exerts more significant therapeutic effect on the brain tissue after nonfatal ischemia. The therapeutic potential for brain edema after fatal stroke is further to be elucidated.

Cerebral ischemia, including stroke, vascular Parkinson's disease and vascular dementia, is one of the most serious medical problems because it causes critical impairment of activity and quality of daily life. Regenerative medicine is now in the spotlight as a promising therapy to treat ischemic brain which has been considered to be irreversible and indicated for no active treatment. Various humoral factors are anticipated for their therapeutic potential for ischemic brain through neurogenic (*e.g.* basic fibroblast growth factor and epidermal growth factor) and angiogenic (*e.g.* vascular endothelial growth factor and hepatocyte growth factor) effects (43–47). Among them, we believe that the vascular hormone AM has several advantages as a therapeutic agent for ischemic brain. We can expect multiple effects of AM through its neuroprotective and vasculo-neuro-regenerative actions as shown in this study. In addition, AM has already been safely used for human patients with heart failure or pulmonary hypertension without any mention of critical adverse effects resulting from iv administration (39).

Thus, we are prompted to propose a new strategy to rescue ischemic brain by using vascular hormone AM for the combined neuroprotective and vasculo-neuro-regenerative therapy to improve impaired neurological function.

## Acknowledgments

This work was supported by grants from Japanese ministry of Education, Culture, Sports, Science and Technology; ministry of Health, Labor and Welfare; and University of Kyoto 21st Century Centers of Excellence program. We thank Dr. Seiichi Hashida (Department of Biochemistry, University of Miyazaki) for measuring mature PAMP; and Dr. Kazuhiko Nozaki and Masaki Nishimura, (Department of Neurosurgery, University of Kyoto) for technical assistance.

Received August 15, 2005. Accepted December 19, 2005.

Address all correspondence and requests for reprints to: Hiroshi Itoh, M.D., Ph.D., Department of Medicine and Clinical Science, Kyoto University Graduate School of Medicine; 54 Shogoin Kawahara-cho, Sakyo-ku, Kyoto 606-8507, Japan. E-mail: hiito@kuhp.kyoto-u.ac.jp.

This work was supported by Japanese ministry of Education, Culture, Sports, Science and Technology; ministry of Health, Labor and Welfare; and University of Kyoto 21st Century Centers of Excellence program.

## References

1. **Kitamura K, Kangawa K, Kawamoto M, Ichiki Y, Nakamura S, Matsuo H, Eto T** 1993 Adrenomedullin: a novel hypotensive peptide isolated from human pheochromocytoma. Biochem Biophys Res Commun 92:553–560
2. **Nagaya N, Mori H, Murakami S, Kangawa K, Kitamura S** 2005 Adrenomedullin: angiogenesis and gene therapy. Am J Physiol Regul Integr Comp Physiol 288:R1432–R1437
3. **Shindo T, Kurihara Y, Nishimatsu H, Moriyama N, Kakoki M, Wang Y, Imai Y, Ebihara A, Kuwaki T, Ju KH, Minamino N, Kangawa K, Ishikawa T, Fukuda M, Akimoto Y, Kawakami H, Imai T, Morita H, Yazaki Y, Nagai R, Hirata Y, Kurihara H** 2001 Vascular abnormalities and elevated blood pressure in mice lacking adrenomedullin gene. Circulation 104:1964–1971
4. **Shimosawa T, Shibagaki Y, Ishibashi K, Kitamura K, Kangawa K, Kato S, Ando K, Fujita T** 2002 Adrenomedullin, an endogenous peptide, counteracts cardiovascular damage. Circulation 105:106–111
5. **Imai Y, Shindo T, Maemura K, Sata M, Saito Y, Kurihara Y, Akishita M, Osuga J, Ishibashi S, Tobe K, Morita H, Oh-hashi Y, Suzuki T, Maekawa H, Kangawa K, Minamino N, Yazaki Y, Nagai R, Kurihara H** 2002 Resistance to neointimal hyperplasia and fatty streak formation in mice with adrenomedullin overexpression. Arterioscler Thromb Vasc Biol 22:1310–1315
6. **Miyashita K, Itoh H, Sawada N, Fukunaga Y, Sone M, Yamahara K, Yurugi-Kobayashi T, Park K, Nakao K** 2003 Adrenomedullin provokes endothelial Akt activation and promotes vascular regeneration both in vitro and in vivo. FEBS Lett 544:86–92
7. **Miyashita K, Itoh H, Sawada N, Fukunaga Y, Sone M, Yamahara K, Yurugi T, Nakao K** 2003 Adrenomedullin promotes proliferation and migration of cultured endothelial cells. Hypertens Res 26:S93–S98
8. **Abe M, Sata M, Nishimatsu H, Nagata D, Suzuki E, Terauchi Y, Kadowaki T, Minamino N, Kangawa K, Matsuo H, Hirata Y, Nagai R** 2003 Adrenomedullin augments collateral development in response to acute ischemia. Biochem Biophys Res Commun 306:10–15
9. **Kim W, Moon SO, Sung MJ, Kim SH, Lee S, So JN, Park SK** 2003 Angiogenic role of adrenomedullin through activation of Akt, mitogen-activated protein kinase, and focal adhesion kinase in endothelial cells. FASEB J 17:1937–1939
10. **Tokunaga N, Nagaya N, Shirai M, Tanaka E, Ishibashi-Ueda H, Harada-Shiba M, Kanda M, Ito T, Shimizu W, Tabata Y, Uematsu M, Nishigami K, Sano S, Kangawa K, Mori H** 2004 Adrenomedullin gene transfer induces therapeutic angiogenesis in a rabbit model of chronic hind limb ischemia: benefits of a novel nonviral vector, gelatin. Circulation 109:526–531
11. **Iwase T, Nagaya N, Fujii T, Itoh T, Ishibashi-Ueda H, Yamagishi M, Miyatake K, Matsumoto T, Kitamura S, Kangawa K** 2005 Adrenomedullin enhances angiogenic potency of bone marrow transplantation in a rat model of hindlimb ischemia. Circulation 111:356–362
12. **Eto T** 2001 A review of the biological properties and clinical implications of adrenomedullin and proadrenomedullin N-terminal 20 peptide (PAMP), hypotensive and vasodilating peptides. Peptides 22:1693–1711
13. **Serrano J, Alonso D, Fernandez AP, Encinas JM, Lopez JC, Castro-Blanco S, Fernandez-Vizarra P, Richart A, Santacana M, Uttenthal LO, Bentura ML, Martinez-Murillo R, Martinez A, Cuttitta F, Rodrigo J** 2002 Adrenomedullin in the central nervous system. Microsc Res Tech 57:76–90
14. **Wang X, Yue TL, Barone FC, White RF, Clark RK, Willette RN, Sulpizio AC, Aiyar NV, Ruffolo Jr RR, Feuerstein GZ** 1995 Discovery of adrenomedullin in rat ischemic cortex and evidence for its role in exacerbating focal brain ischemic damage. Proc Natl Acad Sci USA 92:11480–11484
15. **Dogan A, Suzuki Y, Koketsu N, Osuka K, Saito K, Takayasu M, Shibuya M, Yoshida J** 1997 Intravenous infusion of adrenomedullin and increase in regional cerebral blood flow and prevention of ischemic brain injury after middle cerebral artery occlusion in rats. J Cereb Blood Flow Metab 17:19–25
16. **Watanabe K, Takayasu M, Noda A, Hara M, Takagi T, Suzuki Y, Yoshia J** 2001 Adrenomedullin reduces ischemic brain injury after transient middle cerebral artery occlusion in rats. Acta Neurochir (Wien) 143:1157–1161
17. **Xia CF, Yin H, Borlongan CV, Chao J, Chao L** 2004 Adrenomedullin gene delivery protects against cerebral ischemic injury by promoting astrocyte migration and survival. Hum Gene Ther 15:1243–1254
18. **Hashida S, Kitamura K, Nagatomo Y, Shibata Y, Imamura T, Yamada K, Fujimoto S, Kato J, Morishita K, Eto T** 2004 Development of an ultrasensitive enzyme immunoassay for human proadrenomedullin N-terminal 20 peptide and direct measurement of two molecular forms of PAMP in plasma from healthy subjects and patients with cardiovascular disease. Clin Biochem 37:14–21
19. **Longa EZ, Weinstein PR, Carlson S, Cummins R** 1989 Reversible middle cerebral artery occlusion without craniectomy in rats. Stroke 20:84–91
20. **Teramoto T, Qiu J, Plumier JC, Moskowitz MA** 2003 EGF amplifies the replacement of parvalbumin-expressing striatal interneurons after ischemia. J Clin Invest 111:1125–1132
21. **Venditti A, Battaglia A, Del Poeta G, Buccisano F, Maurillo L, Tamburini A, Del Moro B, Epiceno AM, Martiradonna M, Caravita T, Santinelli S, Adorno G, Picardi A, Zinno F, Lanti A, Bruno A, Suppo G, Franchi A, Franconi G, Amadori S** 1999 Enumeration of CD34+ hematopoietic progenitor cells for clinical transplantation: comparison of three different methods. Bone Marrow Transplant 24:1019–1027
22. **Swanson RA, Morton MT, Tsao-Wu G, Savalos RA, Davidson C, Sharp FR** 1990 A semiautomated method for measuring brain infarct volume. J Cereb Blood Flow Metab 10:290–293
23. **Zhang ZG, Zhang L, Croll SD, Chopp M** 2002 Angiopoietin-1 reduces cerebral blood vessel leakage and ischemic lesion volume after focal cerebral embolic ischemia in mice. Neuroscience 2002 113:683–687

24. **Hayashi H, Ishisaki A, Imamura T** 2003 Smad mediates BMP-2-induced upregulation of FGF-evoked PC12 cell differentiation. FEBS Lett 536:30–34
25. **Iimuro S, Shindo T, Moriyama N, Amaki T, Niu P, Takeda N, Iwata H, Zhang Y, Ebihara A, Nagai R** 2004 Angiogenic effects of adrenomedullin in ischemia and tumor growth. Circ Res 95:415–423
26. **Nakano S, Kogure K, Fujikura H** 1990 Ischemia-induced slowly progressive neuronal damage in the rat brain. Neuroscience 38:115–124
27. **Graham SH, Chen J** 2001 Programmed cell death in cerebral ischemia. J Cereb Blood Flow Metab 21:99–109
28. **Northington FJ, Ferriero DM, Graham EM, Traystman RJ, Martin LJ** 2001 Early neurodegeneration after hypoxia-ischemia in neonatal rat is necrosis while delayed neuronal death is apoptosis. Neurobiol Dis 8:207–219
29. **Stoll G, Jander S, Schroeter M** 1998 Inflammation and glial responses in ischemic brain lesions. Prog Neurobiol 56:149–171
30. **Gilgun-Sherki Y, Rosenbaum Z, Melamed E, Offen D** 2002 Antioxidant therapy in acute central nervous system injury: current state. Pharmacol Rev 54:271–284
31. **Kim W, Moon SO, Lee S, Sung MJ, Kim SH, Park SK** 2003 Adrenomedullin reduces VEGF-induced endothelial adhesion molecules and adhesiveness through a phosphatidylinositol 3′-kinase pathway. Arterioscler Thromb Vasc Biol 23:1377–1383
32. **Kawai J, Ando K, Tojo A, Shimosawa T, Takahashi K, Onozato ML, Yamasaki M, Ogita T, Nakaoka T, Fujita T** 2004 Endogenous adrenomedullin protects against vascular response to injury in mice. Circulation 109:1147–1153
33. **Niu P, Shindo T, Iwata H, Iimuro S, Takeda N, Zhang Y, Ebihara A, Suematsu Y, Kangawa K, Hirata Y, Nagai R** 2004 Protective effects of endogenous adrenomedullin on cardiac hypertrophy, fibrosis, and renal damage. Circulation 109:1789–1794
34. **Krupinski J, Kaluza J, Kumar P, Kumar S, Wang JM** 1994 Role of angiogenesis in patients with cerebral ischemic stroke. Stroke 25:1794–1798
35. **Palmer TD, Willhoite AR, Gage FH** 2000 Vascular niche for adult hippocampal neurogenesis. J Comp Neurol 425:479–494
36. **Louissaint Jr A, Rao S, Leventhal C, Goldman SA** 2002 Coordinated interaction of neurogenesis and angiogenesis in the adult songbird brain. Neuron 34:945–960
37. **Asahara T, Murohara T, Sullivan A, Silver M, van der Zee R, Li T, Witzenbichler B, Schatteman G, Isner JM** 1997 Isolation of putative progenitor endothelial cells for angiogenesis. Science 275:964–967
38. **Taguchi A, Soma T, Tanaka H, Kanda T, Nishimura H, Yoshikawa H, Tsukamoto Y, Iso H, Fujimori Y, Stern DM, Naritomi H, Matsuyama T** 2004 Administration of CD34+ cells after stroke enhances neurogenesis via angiogenesis in a mouse model. J Clin Invest 114:330–338
39. **Nagaya N, Satoh T, Nishikimi T, Uematsu M, Furuichi S, Sakamaki F, Oya H, Kyotani S, Nakanishi N, Goto Y, Masuda Y, Miyatake K, Kangawa K** 2000 Hemodynamic, renal, and hormonal effects of adrenomedullin infusion in patients with congestive heart failure. Circulation 101:498–503
40. **Doi K, Itoh H, Ikeda T, Hosoda K, Ogawa Y, Igaki T, Yamashita J, Chun TH, Inoue M, Masatsugu K, Matsuda K, Ohmori K, Nakao K** 1997 Adenovirus-mediated gene transfer of C-type natriuretic peptide causes G1 growth inhibition of cultured vascular smooth muscle cells. Biochem Biophys Res Commun 239:889–894
41. **Komatsu Y, Itoh H, Suga S, Ogawa Y, Hama N, Kishimoto I, Nakagawa O, Igaki T, Doi K, Yoshimasa T, Nakao K** 1996 Regulation of endothelial production of C-type natriuretic peptide in coculture with vascular smooth muscle cells. Role of the vascular natriuretic peptide system in vascular growth inhibition. Circ Res 78:606–614
42. **Hippenstiel S, Witzenrath M, Schmeck B, Hocke A, Krisp M, Krull M, Seybold J, Seeger W, Rascher W, Schutte H, Suttorp N** 2002 Adrenomedullin reduces endothelial hyperpermeability. Circ Res 91:618–625
43. **Nakatomi H, Kuriu T, Okabe S, Yamamoto S, Hatano O, Kawahara N, Tamura A, Kirino T, Nakafuku M** 2002 Regeneration of hippocampal pyramidal neurons after ischemic brain injury by recruitment of endogenous neural progenitors. Cell 110:429–441
44. **Zhang ZG, Zhang L, Jiang Q, Zhang R, Davies K, Powers C, Bruggen N, Chopp M** 2000 VEGF enhances angiogenesis and promotes blood-brain barrier leakage in the ischemic brain. J Clin Invest 106:829–838
45. **Shimamura M, Sato N, Oshima K, Aoki M, Kurinami H, Waguri S, Uchiyama Y, Ogihara T, Kaneda Y, Morishita R** 2004 Novel therapeutic strategy to treat brain ischemia: overexpression of hepatocyte growth factor gene reduced ischemic injury without cerebral edema in rat model. Circulation 109:424–431
46. **Sun Y, Jin K, Xie L, Childs J, Mao XO, Logvinova A, Greenberg DA** 2003 VEGF-induced neuroprotection, neurogenesis, and angiogenesis after focal cerebral ischemia. J Clin Invest 111:1843–1851
47. **Sondell M, Lundborg G, Kanje M** 1999 Vascular endothelial growth factor has neurotrophic activity and stimulates axonal outgrowth, enhancing cell survival and Schwann cell proliferation in the peripheral nervous system. J Neurosci 19:5731–5740

*Endocrinology* is published monthly by The Endocrine Society (http://www.endo-society.org), the foremost professional society serving the endocrine community.

THE JOURNAL OF BIOLOGICAL CHEMISTRY VOL. 282, NO. 3, pp. 1998–2010, January 19, 2007


# Coactivation of the N-terminal Transactivation of Mineralocorticoid Receptor by Ubc9*

Received for publication, August 14, 2006, and in revised form, October 23, 2006 Published, JBC Papers in Press, November 14, 2006, DOI 10.1074/jbc.M607741200

**Kenichi Yokota[‡], Hirotaka Shibata[‡§1], Isao Kurihara[‡], Sakiko Kobayashi[‡], Noriko Suda[‡], Ayano Murai-Takeda[‡], Ikuo Saito[‡§], Hirochika Kitagawa[¶], Shigeaki Kato[¶], Takao Saruta[‡], and Hiroshi Itoh[‡]**

*From the [‡]Department of Internal Medicine, School of Medicine, and the [§]Health Center, Keio University, Tokyo 160-8582 and the [¶]Institute of Molecular and Cellular Bioscience, University of Tokyo, Tokyo 113-0032, Japan*

Molecular mechanisms underlying mineralocorticoid receptor (MR)-mediated gene expression are not fully understood. Various transcription factors are post-translationally modified by small ubiquitin-related modifier-1 (SUMO-1). We investigated the role of the SUMO-1-conjugating enzyme Ubc9 in MR transactivation. Yeast two-hybrid, GST-pulldown, and coimmunoprecipitation assays showed that Ubc9 interacted with N-terminal MR-(1–670). Endogenous Ubc9 is associated with stably expressing MR in 293-MR cells. Transient transfection assays in COS-1 cells showed that Ubc9 increased MR transactivation of reporter constructs containing *MRE*, *ENaC*, or *MMTV* promoter in a hormone-sensitive manner. Moreover, reduction of Ubc9 protein levels by small interfering RNA attenuated hormonal activation of a reporter construct as well as an endogenous target gene by MR. A sumoylation-inactive mutant Ubc9(C93S) similarly interacted with MR and potentiated aldosterone-dependent MR transactivation. An MR mutant in which four lysine residues within sumoylation motifs were mutated into arginine (K89R/K399R/K494R/K953R) failed to be sumoylated, but Ubc9 similarly enhanced transactivation by the mutant MR, indicating that sumoylation activity is dispensable for coactivation capacity of Ubc9. Coexpression of Ubc9 and steroid receptor coactivator-1 (SRC-1) synergistically enhanced MR-mediated transactivation in transient transfection assays. Indeed, chromatin immunoprecipitation assays demonstrated that endogenous MR, Ubc9, and SRC-1 were recruited to an endogenous *ENaC* gene promoter in a largely aldosterone-dependent manner. Coimmunoprecipitation assays showed a complex of MR, Ubc9, and SRC-1 in mammalian cells, and the endogenous proteins were colocalized in the nuclei of the mouse collecting duct cells. These findings support a physiological role of Ubc9 as a transcriptional MR coactivator, beyond the known SUMO E2-conjugating enzyme.

The human mineralocorticoid receptor (MR,[2] NR3C2), a ligand-dependent transcription factor that belongs to the nuclear receptor superfamily, mediates most of the known effects of aldosterone (1, 2). Besides its involvement in the regulation of electrolyte balance in epithelial cells, most notably in the distal collecting duct of the kidney and the colon, MR is also present in a variety of nonepithelial cells, such as cardiomyocytes and neurons (2–4). Two clinical trials, the Randomized Aldactone Evaluation Study (5) and Eplerenone Post-acute Myocardial Infarction Heart Failure Efficacy and Survival Study (6), shed new light on MR as an important pathogenic mediator of cardiac and vascular remodeling, because treatment with MR antagonist spironolactone or eplerenone was effective in significantly reducing the morbidity and mortality of patients with congestive heart failure. However, molecular mechanisms to account for the successful treatment remain to be elucidated.

MR functions are directed by specific activation domains, designated as activation function 1 (AF-1), which resides in the N terminus, and activation function 2 (AF-2), which resides in the C-terminal ligand-binding domain. Regulation of gene transcription by MR requires the ligand-dependent recruitment of proteins characterized as coactivators (7–12). Among these coactivators, three so-called p160 family coactivators, steroid receptor coactivator-1 (SRC-1) (13, 14), SRC-2, and SRC-3, can interact with most nuclear receptors and are ubiquitously expressed in various tissues. These coactivators have histone acetyltransferase activity to overcome repressive effects of chromatin structure on transcription.

Besides these factors, several coregulators have various enzymatic activities, thus contributing to their abilities to enhance receptor-mediated transcription. The SUMO post-translationally modifies various proteins with roles in diverse processes, including regulation of transcription, chromatin structure, and DNA repair (15–19). Like ubiquitylation, the covalent attach-

* This work was supported by a Grant-in-aid for Scientific Research (C) 17590966, 2005–2006 (to H. S.), from the Japan Society for the Promotion of Science, a grant from Yamaguchi Endocrine Research Association (to H. S.), a grant from the Smoking Research Foundation (to H. I.), an independent research grant from Pfizer Pharmaceuticals Inc. (to H. S.), and a Health Labor Science Research Grant for Disorders of Adrenocortical Hormone Production from the Ministry of Health, Labor, and Welfare, Japan (to H. S.). The costs of publication of this article were defrayed in part by the payment of page charges. This article must therefore be hereby marked "*advertisement*" in accordance with 18 U.S.C. Section 1734 solely to indicate this fact.

[1] To whom correspondence should be addressed. Tel.: 81-3-3353-1211 (ext. 62312); Fax: 81-3-5363-3635; E-mail: hiro-405@cb3.so-net.ne.jp.

[2] The abbreviations used are: MR, mineralocorticoid receptor; GST, glutathione *S*-transferase; SF-1, steroidogenic factor-1; SUMO, small ubiquitin-related modifier; ENaC, epithelial sodium channel; MMTV, mouse mammary tumor virus; SRC-1, steroid receptor coactivator-1; E1, SUMO-activating enzyme; E2, SUMO carrier protein; E3, SUMO-protein isopeptide ligase; IP, immunoprecipitation; Sgk, serum- and glucocorticoid-regulated kinase; p/CIP, p300/CBP cointegrator protein; CBP, cAMP-response element-binding protein-binding protein; EGFP, enhanced green fluorescent protein; DsRed, Discosoma sp. Red; YFP, yellow fluorescent protein; ChIP, chromatin immunoprecipitation; WB, Western blot; DMEM, Dulbecco's modified Eagle's medium; RT, reverse transcription; GAPDH, glyceraldehyde-3-phosphate dehydrogenase; siRNA, small interfering RNA; HA, hemagglutinin.

ment of SUMO to its targets (sumoylation) involves three enzymatic reactions as follows: the SUMO E1-activating, E2-conjugating enzymes, and E3 ligase. The SUMO E1 is a heterodimer of SAE1/SAE2 in mammals (Aos1/Uba2 in yeast). In contrast to the ubiquitin system where dozens of E2 enzymes have been identified, sumoylation uses only a single E2 enzyme, Ubc9. SUMO-1 is conjugated to target proteins at the consensus sequence $\psi KXE$ (where $\psi$ is any hydrophobic amino acid, and $X$ is any amino acid). Three unrelated proteins have SUMO E3 ligase activity to promote transfer of SUMO from E2 to specific substrates as follows: the protein inhibitor of activated signal transducer and activator of transcription 1 (PIAS1) protein (20–22), RanBP2 (23, 24), and polycomb group protein Pc2 (25).

Considerable numbers of nuclear receptors, including glucocorticoid receptor (26–30), androgen receptor (21, 22, 31–36), progesterone receptor (36, 37), MR (38), estrogen receptor $\alpha$ (39), peroxisome proliferator-activated receptor $\gamma$ (40–42), and SF-1 (43–45), are modified by SUMO through a series of enzyme reactions, and sumoylation of the receptors mostly resulted in repression of the receptor-dependent transcription. In this study, we focused on the protein-protein interaction between Ubc9 and MR. We describe a new function of Ubc9 as a coactivator of MR by formation of a complex with N-terminal MR and SRC-1 beyond the known SUMO E2-conjugating enzyme, although sumoylation of MR repressed the receptor-dependent transactivation.

## EXPERIMENTAL PROCEDURES

*Antibodies*—Goat anti-human MR (N-17) antibody, goat anti-human SRC-1 (M-341) antibody, and normal goat IgG were obtained from Santa Cruz Biotechnology. Mouse monoclonal anti-Xpress IgG was obtained from Invitrogen. Mouse anti-Ubc9 antibody was obtained from Pharmingen. Rabbit anti-HA antibody was obtained from Clontech. Mouse anti $\alpha$-tubulin antibody was obtained from Oncogene.

*Cell Culture, Transfections, and Luciferase Assays*—COS-1 cells, COS-7 cells, and HEK293 cells were routinely maintained in DMEM (Invitrogen) supplemented with 10% fetal bovine serum (Invitrogen). Twenty four hours before transfection, $5 \times 10^4$ cells per well of a 24-well dish were plated in the medium. All transfections were carried out by using Lipofectamine 2000 (Invitrogen) with 0.3 $\mu$g/well of the luciferase reporter, 0.01 $\mu$g/well of pRL-null internal control plasmids, and the indicated amounts of expression plasmids according to the manufacturer's instructions. After 18–24 h, the medium was changed to DMEM with 10% fetal bovine serum and $10^{-8}$ M aldosterone or vehicle. After an additional 24 h, cell extracts were assayed for both Firefly and *Renilla* luciferase activities with a dual-luciferase reporter assay system (Promega). Relative luciferase activity was determined as ratio of Firefly/Renilla luciferase activities, and data were expressed as the mean (±S.D.) of triplicate values obtained from a representative experiment that was independently repeated at least three times.

*Generation of Human MR Expressing Cell Line, 293-MR*—Human 293F embryonic kidney cells and transformants were routinely maintained in DMEM (Invitrogen) supplemented with 10% fetal bovine serum (Hyclone, UT). To establish stable transformants (293-MR cells), parent 293F cells were transfected with pNTAP-hMR (Stratagene) with Lipofectamine Plus reagents (Invitrogen) and cultured for 2 weeks in the presence of 700 $\mu$g/ml G418 for transformant selection as described previously (46–48). Individual colonies were selected and expanded for further analysis.

*Plasmid Constructs*—Several Ubc9 constructs, such as pcDNA3.1/His-Ubc9, pcDNA3.1/His-Ubc9(C93S), pGADT7-Ubc9, pGEX4T-1-Ubc9, pGEX4T-1-Ubc9(C93S), and pEGFP-Ubc9 were described previously (49, 50). pCMV-YFP-SRC-1 was a generous gift from Dr. Toshihiko Yanase (Kyushu University). 3xMRE-E1b-Luc and pCR3.1-SRC-1 were generous gifts from Dr. Bert W. O'Malley (Baylor College of Medicine, Houston). pGL3-MMTV (−1146/+88)-Luc was a generous gift from Dr. Jorma J. Palvimo (University of Helsinki, Finland). pRShMR was a generous gift from Dr. Ronald M. Evans (The Salk Institute for Biological Studies). pcDNA-HA-SUMO-1 was a generous gift from Dr. Ronald T. Hay (University of St. Andrews). pGL3-ENaC(−1388/+55)-Luc (51) was a generous gift from Dr. Christie P. Thomas (University of Iowa College of Medicine). Several MR fragments, such as MR-(1–984), -(1–670), and -(671–984), were subcloned into pGBKT7, pcDNA3.1/His, and pDsRed vectors using a PCR amplification with primers containing oligonucleotide linkers of restriction enzyme sites. In detail, each MR fragment was first obtained by PCR amplification with primers containing oligonucleotide linkers of restriction enzyme sites (SmaI-SalI for pGBKT7, KpnI-XhoI for pcDNA3.1/His, and XhoI-XmaI for pDsRed), followed by TA cloning into pCRII-TOPO vector (Invitrogen). These pCR-TOPO-MR constructs were then digested with SmaI-SalI, KpnI-XhoI, or XhoI-XmaI and subcloned into the pGBKT7 yeast expression vector (Clontech), pcDNA3.1/His, or pDsRed2-C1 (Clontech) mammalian expression vector (Invitrogen). pRShMR-KRmut, in which the lysine residues positioned at 89, 399, 494, and 953 amino acids were substituted for arginine residues, was generated by the QuickChange site-directed mutagenesis kit (Stratagene). DNA sequencing of all the constructs was confirmed by ABI PRISM dye terminator cycle sequencing analysis (Amersham Biosciences).

*Yeast Two-hybrid Assay*—Yeast two-hybrid assays were used to determine interaction of MR with Ubc9. Yeast Y187 cells were transformed with yeast expression plasmids encoding hMR and Ubc9. $\beta$-Galactosidase activity in liquid culture was determined with chlorophenol red $\beta$-D-galactopyranoside as described previously (49, 50, 52, 53).

*Glutathione S-transferase Pulldown Assay*—Glutathione S-transferase (GST) (pGEX4T-1) protein, GST-Ubc9 (pGEX4T-1-Ubc9), and GST-Ubc9(C93S) (pGEX4T-1-Ubc9(C93S)) fusion proteins were expressed and extracted in *Escherichia coli* DH5$\alpha$ as described previously (49, 52). GST pulldown assay was performed as described (49, 52), with modifications: 50 $\mu$l of glutathione-Sepharose beads 4B (Amersham Biosciences) stored in beads incubation buffer (50 mM potassium phosphate buffer (pH 7.4), 100 mM NaCl, 1 mM $MgCl_2$, 10% glycerol, and 0.1% Tween 20) were incubated with bacterial extracts containing GST fusion proteins together with beads incubation buffer for 30–60 min at room temperature. Preparation of bacteria extracts containing GST fusion protein was as described previ-

ously (49, 52). The supernatant was then removed, and the beads were washed three times with beads incubation buffer. *In vitro*-translated $^{35}$S-labeled proteins were obtained by using TNT Coupled Reticulocyte Lysate Systems (Promega). Crude lysates were incubated with the beads in 200 μl of beads incubation buffer for 60 min at 4 °C with a circle rotator. Finally the beads were washed five times with 1 ml of beads incubation buffer, and the proteins were solubilized in SDS loading buffer and analyzed on SDS-PAGE (12.5% polyacrylamide gel). The input lanes contained 20% of the labeled protein used for binding.

*Western Blot Analysis and Coimmunoprecipitation*—The cells were lysed with lysis buffer (10 mM Tris-HCl (pH 8.0), 150 mM NaCl, 1% Triton X-100, 5 mM EDTA, 2 mM phenylmethylsulfonyl fluoride), and Western blots were performed before the immunoprecipitation (IP) steps to confirm protein expression by corresponding antibodies as described previously (49, 50). The same samples for the Western blots were diluted to 1 ml in IP buffer (20 mM Tris-HCl (pH 7.5), 150 mM NaCl, 10 mM dithiothreitol, 5 ng/μl aprotinin, 0.5 mM phenylmethylsulfonyl fluoride, 0.1% Tween 20) and precleared with protein G plus-agarose beads (Santa Cruz Biotechnology, Santa Cruz, CA), and antibodies were added for 1 h. Immune complexes were adsorbed to protein G plus-agarose beads and washed four times in IP buffer. Proteins were then separated on 12.5% polyacrylamide gels and transferred onto Hybond ECL nitrocellulose membranes (Amersham Biosciences). The primary antibodies used for immunoprecipitation were anti-MR (Santa Cruz Biotechnology) or anti-Xpress (Invitrogen) antibodies, and antibodies used for the Western blots were anti-MR, anti-Xpress, anti-HA (Oncogene), and anti-SRC-1 (Santa Cruz Biotechnology) antibodies.

*RNA Interference*—COS-7 cells were transfected with siRNAs, and luciferase assays were performed as described previously (50). COS-7 cells were plated into 24-well plates, grown until reaching 70–80% confluence, and transfected with 30 pmol of negative control sequence, Ubc9-specific siRNA duplex using Lipofectamine 2000 (Invitrogen) following the manufacturer's instructions. Whole cell extracts were prepared as described previously as follows: siRNA Ubc9#1 sense, 5′-GGC CAG CCA UCA CAA UCA ATT-3′; siRNA Ubc9#1 antisense, 5′-UUG AUU GUG AUG GCU GGC CTC-3′; siRNA Ubc9#2 sense, 5′-GGA ACU UCU AAA UGA ACC ATT-3′; siRNA Ubc9#2 antisense, 5′-UGG UUC AUU UAG AAG UUC CTG-3′; and Silencer Negative Control #1 siRNA (Ambion) were used.

*Chromatin Immunoprecipitation (ChIP) Assay*—ChIP assay was performed as described previously (50). The cross-linked sheared chromatin solution was used for immunoprecipitation with 3 μg of anti-MR (N-17) antibody (Santa Cruz Biotechnology), anti-Ubc9 antibody (Pharmingen), or normal IgG. The immunoprecipitated DNAs were purified by phenol/chloroform extraction, precipitated by ethanol, and amplified by PCR using primers flanking the MRE region or control region as follows: ENaC MRE sense primer, 5′-TTC CTT TCC AGC GCT GGC CAC-3′ (−1567/−1547); ENaC MRE antisense primer, 5′-CCT CCA ACC TTG TCC AGA CCC-3′ (−1317–1297); ENaC control sense primer, 5′-ATG GGC ATG GCC AGG-3′ (+1/+15); ENaC control antisense primer, 5′-CCT GCT CCT CAC GCT-3′ (+251/+265). DNA samples with serial dilution were amplified by PCR to determine the linear range for the amplification (data not shown).

*Immunohistochemical Staining*—Tissues were isolated from 2-month-old wild type male mice, fixed in 4% paraformaldehyde overnight at 4 °C, dehydrated in graded ethanol, and then processed for paraffin embedding. Sections (7 μm) were incubated for 2 h in blocking buffer, which is constituted by 1% bovine serum albumin, 5% normal donkey serum, 20 μg/ml donkey anti-mouse IgG Fab fragment (Jackson ImmunoResearch, West Grove, PA), and 0.02% Triton X-100 in phosphate-buffered saline, and followed by incubation with the primary antibodies overnight at 4 °C. Primary antibodies used in this experiment were as follows: mouse anti-MR, rabbit anti-Ubc9 (Santa Cruz Biotechnology), and rabbit anti-SRC-1 (Santa Cruz Biotechnology), and the optimized dilutions were 1:50–1:100. After incubation with the combination of primary antibodies (MR and Ubc9, MR and SRC-1), slides were incubated with Alexa Fluor 488-conjugated donkey anti-mouse IgG and Alexa Fluor 594-conjugated donkey anti-rabbit IgG (Molecular Probes, Eugene, OR) for 30 min at 4 °C. 4′,6-Diamino-2-phenylindole (DAPI) was used for nuclear staining.

*Fluorescence Imaging*—The images of EGFP-tagged Ubc9 and YFP-tagged SRC-1 were described previously (49, 54). HEK293 cells were transiently transfected with expression vectors of pDsRed-MR with pEGFP-Ubc9 or pYFP-SRC-1. Live cell microscopy of DsRed fusion, EGFP fusion, or YFP fusion proteins was performed on a confocal microscope (Axiovert 100 M, Carl Zeiss Co., Ltd.). Imaging for DsRed and EGFP or YFP was performed by excitation with 543 and 488 nm, respectively, from an argon laser, and the emissions were viewed through band passes ranging from 550 to 600 and 500–550 nm, respectively, by band pass regulation with LSM510 (Carl Zeiss Co., Ltd.). All images were processed as tagged image file format (TIFF) files on Photoshop 7.0 using standard image-processing techniques.

*Semiquantitative RT-PCR*—The effect of endogenous Ubc9 on the endogenous Sgk, Ubc9, and GAPDH levels in the presence of $10^{-8}$ M aldosterone was investigated by semiquantitative RT-PCR. For semiquantitative RT-PCR, total RNA was extracted from 293-MR cells and reverse-transcribed as described previously. Procedures of RT-PCR were performed as described previously elsewhere. Preliminary experiments were conducted to ensure linearity for the semiquantitative procedures. Hot start PCR was performed by heat-activating AmpliTaq Gold DNA polymerase (PerkinElmer Life Sciences) at 94 °C for 4 min. Optimized cycling condition was 30 cycles (for Sgk) or 20 cycles (for Ubc9 and glyceraldehyde-3-phosphate dehydrogenase) for 1 min at 94 °C, 1 min at 55 °C, and 1 min at 72 °C. Oligonucleotide primers were constructed from the published cDNA sequences of Sgk, Ubc9, and GAPDH cDNA. The sequences of the primers were as follows: Sgk sense, 5′-TGG GAT GAT CTC ATT-3′ (1078–1092), and Sgk antisense, 5′-AAA GCC TAG GAA AGC-3′ (1249–1263); Ubc9 sense, 5′-GAG CGA AGG GTA CAC ATT-3′ (1–18), and Ubc9 antisense, 5′-TTC ATG TCG GGG ATC GCC-3′ (250–267); GAPDH sense, 5′-CCC ATC ACC ATC TTC CAG GAG-3′

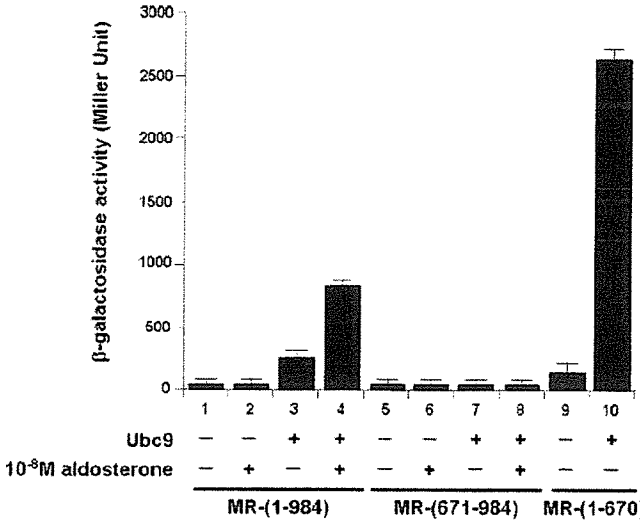


FIGURE 1. **Interaction of Ubc9 with human MR in yeast two-hybrid assays.** Interactions of Ubc9 with full-length (1–984), C-terminal domain (671–984), or N-terminal domain (1–670) of MR were determined in the presence and absence of $10^{-8}$ M aldosterone in yeast two-hybrid assays. β-Galactosidase activity was assayed in liquid cultures in three separate experiments, each with triplicate samples. Values were expressed as the average Miller units (±S.D.) of triplicate values.

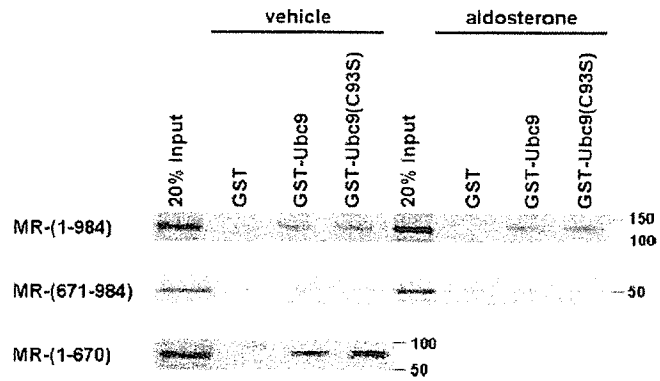


FIGURE 2. **Ubc9 interacts directly with N-terminal MR-(1–670) but not C-terminal MR-(671–984) in GST-pulldown assays.** Ubc9 and Ubc9(C93S) were expressed as GST fusion proteins in *E. coli*. These proteins were coupled to glutathione-Sepharose and incubated with full-length (1–984), C-terminal domain (671–984), or N-terminal domain (1–670) of MR protein that was translated and $^{35}$S-labeled *in vitro* in the presence and absence of $10^{-8}$ M aldosterone. Bound materials as well as 20% of the input were analyzed by SDS-PAGE and autoradiography.

(211–231), and GAPDH antisense, 5′-GTT GTC ATG GAT GAC CTT GGC-3′ (475–495). The predicted sizes of the amplified Sgk, Ubc9, and GAPDH cDNA products were 186, 230, and 285 bp, respectively.

*Statistics*—All experiments were performed in triplicate several times. The *error bars* in the graphs of individual experiments correspond to the S.D. of the triplicate values.

## RESULTS

*Characterization of the Ubc9-MR Protein Interaction*—We have recently shown that nuclear orphan receptor chicken ovalbumin upstream promoter-transcription factor I activates human *CYP11B2* gene transcription in cooperation with Ubc9 and PIAS1, thus resulting in aldosterone secretion in the adrenal zona glomerulosa cells (49, 50). During the studies, we found that Ubc9 also markedly interacts with MR. We therefore described functional interaction of Ubc9 with MR in this study. Yeast β-galactosidase liquid assays were performed to examine interaction of MR with Ubc9. The full-length human MR encoding amino acids 1–984 interacted with Ubc9 in the absence of hormone, and the interaction was significantly enhanced in the presence of $10^{-8}$ M aldosterone (Fig. 1, *lanes 3* and *4*). The ligand-binding domain of MR encoding amino acids 671–984 did not interact with Ubc9 in the absence or presence of aldosterone (Fig. 1, *lanes 7* and *8*). On the other hand, the N-terminal fragment of MR encoding amino acids 1–670 markedly interacted with Ubc9 (Fig. 1, *lanes 9* and *10*). These data indicate that Ubc9 interacts with the N-terminal MR in an aldosterone-sensitive manner.

To confirm this interaction biochemically, we performed GST-pulldown assays using GST-Ubc9 protein and *in vitro* translated [$^{35}$S]Met-labeled MR. The full-length MR-(1–984) interacted with GST-Ubc9 both in the absence and presence of aldosterone but not with GST alone (Fig. 2, *upper panel*). Remarkably, the N-terminal MR-(1–670) strongly interacted with GST-Ubc9 (Fig. 2, *lower panel*); however, the ligand-binding domain of MR-(671–984) showed no interaction with Ubc9 (Fig. 2, *middle panel*). These *in vitro* interaction data are compatible with those in yeast cells. Furthermore, a sumoylation-inactive mutant Ubc9(C93S) similarly interacted with the full-length as well as N-terminal MR (Fig. 2, *upper* and *lower panels*), indicating that sumoylation activity is dispensable for interaction of Ubc9 with MR.

To analyze the physical interaction between MR and Ubc9 in mammalian cells, coimmunoprecipitation assays were performed. Mammalian expression plasmids of MR and Xpress-tagged Ubc9 were transfected into HEK293 cells. Proteins precipitated with anti-MR antibody were resolved by SDS-PAGE, and Western blot using anti-Xpress antibody was conducted. The coimmunoprecipitation experiments clearly showed that both N-terminal (residues 1–670) and full-length MR were associated with Ubc9 (Fig. 3, *A, lane 2,* and *B, lane 2*). In addition, both wild type- and sumoylation-inactive mutants of Ubc9 (C93S) were associated with MR at similar levels (Fig. 3*B, lanes 2* and *3*). To investigate physiological relevance of these observations, we have generated MR stable transformants of 293-MR cells. Although HEK293F cells express no MR, a significant level of expression of MR protein was shown in 293-MR cells by Western blot and coimmunoprecipitations (Fig. 3*C, upper panel*). We were able to show a significant interaction of endogenous Ubc9 with stably expressing MR in 293-MR cells (Fig. 3*C, lower panel*). Taken together with the interaction data in yeast cells, *in vitro,* and mammalian cells, Ubc9 interacts with the N-terminal region of MR.

*Ubc9 Functions as a Coactivator of MR-mediated Transactivation in an Agonist-dependent Manner*—To address functional effects of interaction between MR and Ubc9, transient transfection assays were performed. Transfection of human MR cDNA expression plasmid significantly activated three reporter constructs containing 3xMRE, ENaC, or MMTV in an aldosterone-dependent manner in COS-1 cells (Fig. 4*A, lanes 6, 13,* and *20*). Coexpression of Ubc9 potentiated MR-mediated

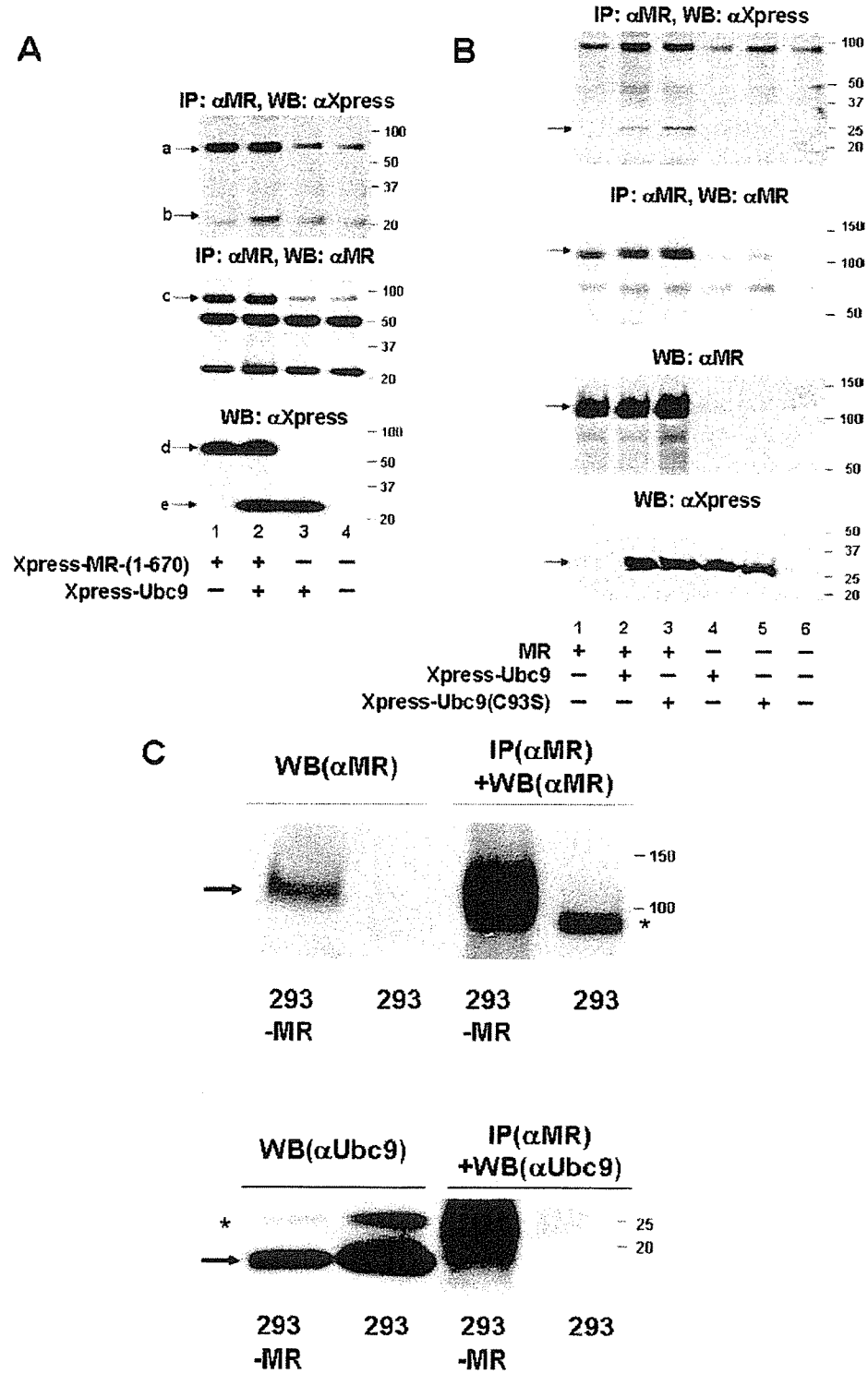


FIGURE 3. **Ubc9 is associated with MR in mammalian cells.** *A*, HEK293 cells were transfected with Xpress-tagged MR-(1–670) and/or Xpress-tagged Ubc9, and the amount of DNA was kept constant by the addition of empty expression vectors. Whole cell extracts were subjected to immunoprecipitation (*IP*) with anti-MR antibody, and immunoprecipitates were subsequently analyzed by Western blotting (*WB*) with anti-Xpress antibody (*top panel*) or anti-MR antibody (*middle panel*). Levels of corresponding proteins were determined by Western blotting with anti-Xpress antibody (*bottom panel*). *Arrows a–e* correspond to Xpress-MR-(1–670), Xpress-Ubc9, MR-(1–670), Xpress-(1–670), and Xpress-Ubc9, respectively. *B*, HEK293 cells were transfected with MR-(1–984) with Xpress-tagged wild type or C93S mutant of Ubc9, and the amount of DNA was kept constant by the addition of empty expression vectors. Whole cell extracts were subjected to IP with anti-MR antibody, and immunoprecipitates were subsequently analyzed by WB with anti-Xpress antibody (*top panel*) or anti-MR antibody (*2nd panel*). Levels of corresponding proteins were determined by WB with anti-MR (*3rd panel*) or anti-Xpress antibody (*bottom panel*). *C*, to investigate interaction of stably expressing MR with endogenous Ubc9, 293-MR cells were utilized. HEK293 cells were used as a control that expresses no MR protein. Both Western blotting and coimmunoprecipitation clearly showed that MR was expressed in 293-MR cells but not in HEK293 cells (*upper panel*). Whole cell extracts from 293-MR or HEK293 cells were subjected to IP with anti-MR antibody, and immunoprecipitates were subsequently analyzed by WB with anti-Ubc9 antibody (*lower panel*). * indicates nonspecific protein.

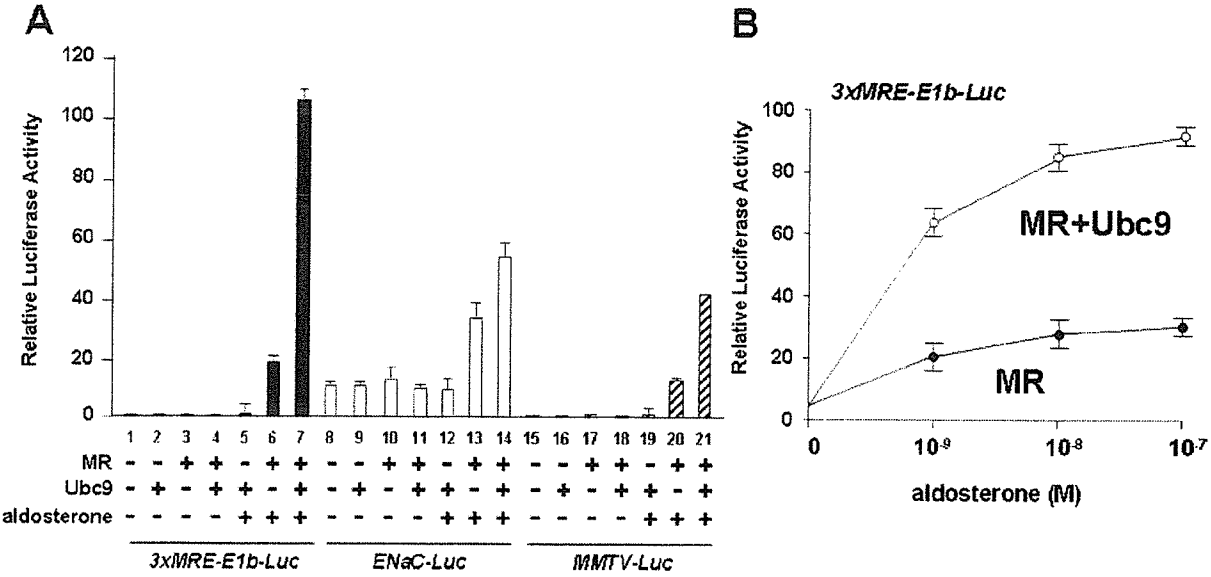


FIGURE 4. **Ubc9 enhances MR-mediated transcriptional activities of three reporter genes in COS-1 cells.** *A*, Ubc9 enhanced aldosterone-induced MR transactivation of reporter genes, *3xMRE-E1b*-Luc, *ENaC*-Luc, and *MMTV*-Luc in COS-1 cells. COS-1 cells were transfected with 0.61 $\mu$g of total DNA, including 0.1 $\mu$g of empty vector (pRS) or MR (pRShMR) and 0.2 $\mu$g of Ubc9 construct, 0.01 $\mu$g of phRL-null with 0.3 $\mu$g of *3xMRE-E1b*-luciferase (*3xMRE-E1b-Luc*), *ENaC-(−1388/+55)*-luciferase (*ENaC-Luc*), and *MMTV-(−1146/+88)*-luciferase (*MMTV-Luc*) reporter DNA for each well of the 24-well dish indicated. Forty eight hours post-transfection, cells were harvested, and the extracts were assayed for luciferase activity. Assays were performed in three separate experiments, each with triplicate samples. *B*, Ubc9 modulation of aldosterone-mediated MR transactivation properties in a concentration-dependent manner. COS-1 cells were transfected with 0.61 $\mu$g of total DNA, including 0.1 $\mu$g of MR plasmid (pRShMR), 0.01 $\mu$g of phRL-null, and 0.3 $\mu$g of *3xMRE-E1b-Luc* reporter with 0.2 $\mu$g of empty (pcDNA3.1/His) or Ubc9 (pcDNA3.1/His-Ubc9) plasmid. Twenty four hours post-transfection, cells were treated with vehicle, $10^{-9}$, $10^{-8}$, or $10^{-7}$ M aldosterone, and cells were harvested at 48 h post-transfection, and the extracts were assayed for luciferase activity. Assays were performed in three separate experiments, each with triplicate samples.

transactivation of the reporter constructs in the presence of aldosterone (Fig. 4*A*, *lanes 7, 14,* and *21*); however, the extent of potentiation by ectopic expression of Ubc9 varied depending on the reporter construct. Overexpression of Ubc9 alone had no significant effects on these reporter activities (Fig. 4*A*, *lanes 5, 12,* and *19*), indicating that the ability of Ubc9 in enhancing MR-mediated transactivation is dependent on interaction with MR. In addition, increasing concentrations of aldosterone treatment activated MR-mediated transactivation, and coexpression of Ubc9 significantly enhanced its transactivation (Fig. 4*B*), indicating that Ubc9 potentiates MR-dependent transactivation in an aldosterone concentration-dependent manner. The increase in reporter activity was not because of increased cellular concentration of MR, because Western blot did not reveal alterations in immunoreactive MR protein content (Fig. 3*B*, *2nd* and *3rd panels* in *lanes 1* and *2*). These findings indicate that Ubc9 has transcriptional coactivator capacity of MR *in vivo*. We next tested effects of ligands on Ubc9's ability in MR-mediated transcription. To examine the influence of the nature of the ligand on MR responses to Ubc9, experiments performed with cortisol but not spironolactone led to the same potentiating effects (data not shown). These results indicate that a particular ligand-binding domain conformation induced by the nature of the bound agonistic ligand is crucial for Ubc9 action on MR and thus is presumably dependent on the AF-2.

*Endogenous Ubc9 Is Required for MR-mediated Transactivation*—If Ubc9 functions as a coactivator of MR, reducing the endogenous level of Ubc9 should decrease the transcriptional activity by MR in transient transfection assays. As described previously (Fig. 4*A*), overexpression of MR activated 3xMRE-E1b-Luc reporter activity by 20-fold. Cotransfection of two sets of Ubc9 siRNA (siRNA-Ubc9#1 or siRNA-Ubc9#2), but not negative control (siRNA-Control), effectively reduced the endogenous levels of Ubc9 protein but had no effect on the $\alpha$-tubulin protein level as shown in Western blot (Fig. 5*B*). Reduction of endogenous Ubc9 protein level decreased the MR-mediated transactivation by 63% (siRNA-Ubc9#1) (Fig. 5*A*, *lane 7*) and 37% (siRNA-Ubc9#2) (Fig. 5*A*, *lane 8*) in the presence of aldosterone but not in the absence (Fig. 5*A*, *lanes 1–4*). We also examined the effect of reducing endogenous Ubc9 on aldosterone-dependent activation of the *Sgk* gene in 293-MR cells. In a typical experiment siRNA against Ubc9 lowered endogenous levels of *Ubc9* mRNA by about 90%, compared with cells receiving a control siRNA (Fig. 6, *A*, *lower panel,* and *B*). The addition of the MR agonist aldosterone caused strong induction of *Sgk* mRNA levels by 3.5-fold, indicating that the stably expressing MR protein functions physiologically (Fig. 6, *A* and *C*). The siRNA against Ubc9 lowered the aldosterone-induced level of *Sgk* mRNA by 48%, as compared with the level by introduction of control siRNA (Fig. 6, *A* and *C*, *lanes 3* and *4*). The *Ubc9* and *Sgk* mRNA levels were normalized to *GAPDH* mRNA levels, thus demonstrating that the effects of the Ubc9-directed siRNA were gene-specific. Thus, although many different coactivators are involved in mediating transcriptional activation by MR, endogenous Ubc9 is necessary for efficient induction of the endogenous *Sgk* gene in response to hormones. These findings indicate that endogenous Ubc9 normally functions as a transcriptional coactivator for the MR-mediated transactivation.

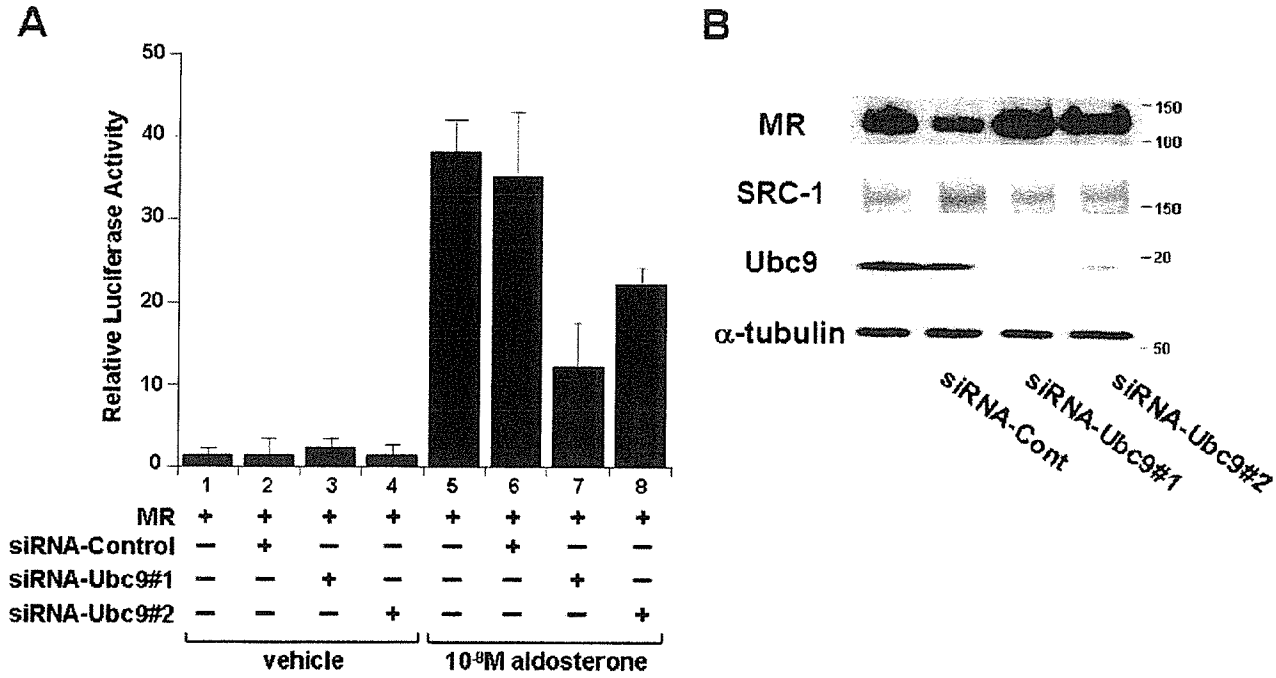


FIGURE 5. **Endogenous Ubc9 is required for MR-mediated transactivation.** *A*, knockdown of the Ubc9 protein reduces the MR-mediated transcription of the *3xMRE-E1b-Luc* reporter construct. COS-7 cells in 24-well dishes were transiently transfected using Lipofectamine 2000 with 0.41 $\mu$g of total DNA, including 0.1 $\mu$g of MR, 0.01 $\mu$g of phRL-null, and 0.3 $\mu$g of *3xMRE-E1b-Luc* reporter DNA, and 20 pmol of either Ubc9#1, Ubc9#2, or negative control siRNA duplex, as indicated. Forty eight hours post-transfection of siRNA, plasmid DNAs were consecutively transfected, and cells were treated with $10^{-8}$ M aldosterone at 24 h after DNA transfection. Ninety six hours post-transfection, cells were harvested, and luciferase reporter assays were performed according to the manufacturer's instructions. *B*, Western blot analysis of endogenous Ubc9 protein level that was efficiently reduced by transfection of either Ubc9-specific siRNA duplex (*siRNA-Ubc9#1* or *siRNA-Ubc9#2*) but not of negative control siRNA duplex (*siRNA-Control*).

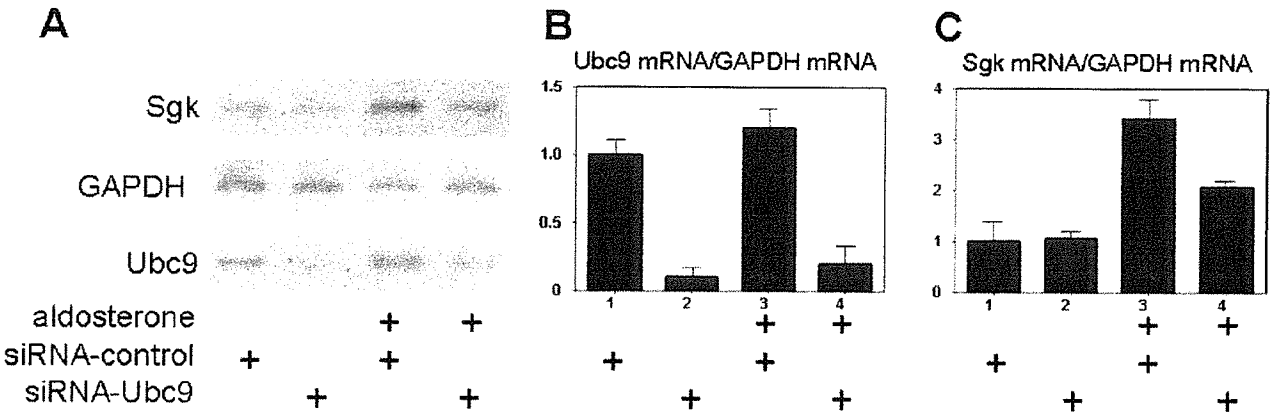


FIGURE 6. **Ubc9 is necessary for efficient transcriptional activation by MR.** siRNA against Ubc9 or control siRNA was transfected into 293-MR cells. After growth with or without $10^{-8}$ M aldosterone, cDNA was synthesized from total RNA and analyzed by semiquantitative RT-PCR. The level of Sgk mRNA or Ubc9 mRNA was normalized to that of GAPDH; all ratios are expressed relative to the vehicle and siRNA control (*lane 1*). Statistical significance was calculated using an unpaired *t* test on three independent experiments. 293-MR cells were treated with siRNA and $10^{-8}$ M aldosterone.

*Modification of MR by SUMO-1*—SUMO-1 modification of transcription factors, including nuclear hormone receptors, is known to affect transcriptional activity, and we therefore examined whether MR is a substrate for SUMO-1 modification. MR displays several sumoylation consensus motifs, previously described as synergy control motifs (55). We generated a mutant MR construct in which four lysine residues within sumoylation consensus motifs were mutated into arginine, K89R/K399R/K494R/K953R, designated as KRmut MR by site-directed mutagenesis. The ability of wild type and KRmut MR proteins to undergo SUMO-1 modifications was analyzed by *in vivo* sumoylation assays as described previously (38). The wild type- and KRmut-MR with or without HA-tagged SUMO-1 were transfected into HEK293 cells. Whole cell extracts from transfected HEK293 cells were immunoprecipitated with anti-MR antibody, followed by immunoblotting with anti-HA or anti-MR antibody (Fig. 7). The results showed that the slower migrating multiple bands were detected only when HA-SUMO-1 and wild type MR were coexpressed (Fig. 7, *lane 2*). Interestingly, sumoylation of MR appeared to be decreased in the presence of aldosterone than in the absence for unknown mechanisms (Fig. 7, *top panel, lanes 2* and *4*). When HA-SUMO-1 and KRmut MR were coexpressed, these high molecular weight protein bands were almost disrupted (Fig. 7,

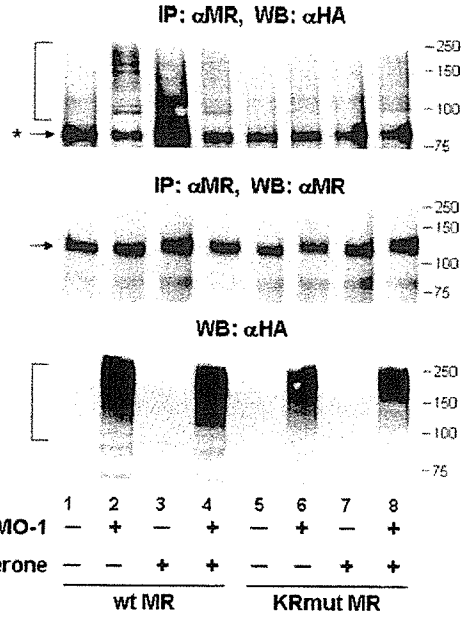


FIGURE 7. ***In vivo* sumoylation of hMR.** The wild type- but not KRmut-hMR (K89R/K399R/K494R/K953R) was sumoylated in HEK293 cells. HEK293 cells were transfected with wild type (pRShMR) or KRmut MR (pRShMR-KRmut) and SUMO-1 (pcDNA3-HA-SUMO-1). Twenty four hours post-transfection, cells were treated with $10^{-8}$ M aldosterone or vehicle (ethanol). Forty eight hours post-transfection, cells were harvested. Whole cell extracts were IP with anti-MR antibody, and immunoprecipitates were subsequently analyzed by WB with anti-HA (*top panel*) or anti-MR (*2nd panel*) antibody. Levels of expression of SUMO-1 (*bottom panel*) were determined by WB with anti-MR and anti-HA antibodies, respectively. *Brackets* showed sumoylated MR (*top panel*) and multiple sumoylated proteins (*bottom panel*). * indicates nonspecific protein (*top panel*).

*lanes 5–8*), suggesting that Lys-89, Lys-399, Lys-494, and Lys-953 are the main sumoylation sites of MR.

*Ubc9 Potentiates MR-mediated Transcription Independent of Sumoylation Activity*—To elucidate whether E2 SUMO-1-conjugating enzyme activity of Ubc9 is required for coactivation of MR, transient transfection assays were performed utilizing the sumoylation-inactive mutant Ubc9 (C93S). Coexpression of Ubc9 (C93S) potentiated the transcriptional activity of wild type MR by 4-fold (Fig. 8*A*, *lane 6 versus lane 4*) in a similar manner to coexpression of wild type Ubc9 (Fig. 8*A*, *lane 5 versus lane 4*). The transcriptional properties of KRmut MR on 3xMRE-E1b-Luc reporter activity showed enhanced transcriptional activities by ~5-fold (Fig. 8*A*, *lane 10 versus lane 4*) compared with the wild type MR. This finding was also supported by data that overexpression of SENP1, a SUMO-1 isopeptidase, similarly potentiated MR-mediated transactivation (data not shown). Therefore, sumoylation of MR is likely to repress its transcriptional activities as shown previously (38). Coexpression of Ubc9 or Ubc9 (C93S) further potentiated the KRmut MR-mediated transactivation by 3-fold (Fig. 8*A*, *lanes 10–12*). These findings suggest that sumoylation activity of Ubc9 is not necessary for enhancement of MR-mediated transcription. Because KRmut MR displayed stronger transactivation than wild type MR, it is tempting to test whether interaction of MR with Ubc9 was affected. The coimmunoprecipitation assays showed that wild type- as well as KRmut-MR similarly interacted with Xpress-tagged Ubc9 (Fig. 8*B*, *top panel, lanes 2* and *3*), indicating that interaction between MR and Ubc9 is not altered depending upon sumoylation status of MR. Similarly, both Ubc9 and Ubc9 (C93S) equally interacted with MR (Figs. 2 and 3*B*), indicating that interaction between MR and Ubc9 is not altered depending upon sumoylation activity of Ubc9.

*Ubc9 and SRC-1 Synergistically Potentiated MR-mediated Transcription*—Ubc9 is a strict ligand-dependent coactivator of MR, but Ubc9 does not directly interact with the ligand-binding domain of MR. Therefore, it is tempting to test that Ubc9 is associated with certain coactivators interacting with MR AF-2 domain. We investigated the combined effects of Ubc9 and several known AF-2 coactivators on MR-mediated transcription in transient transfection assays. Among several known AF-2 coactivators, we found that SRC-1, but not p/CIP or CBP/p300 (data not shown), synergistically potentiated MR-mediated transactivation in cooperation with Ubc9. As shown in Fig. 9, overexpression of either SRC-1 (*lanes 5–7*) or Ubc9 (*lanes 8–10*) in cells enhanced aldosterone-induced MR-dependent transcription by ~4-fold (Fig. 9, *lanes 7* and *10*), compared with untransfected cells (Fig. 9, *lane 4*) in a dose-dependent manner. When both Ubc9 and SRC-1 were overexpressed in cells, reporter gene activity was synergistically elevated to levels 12–13-fold higher than in untransfected cells (Fig. 9, *lanes 13* and *16 versus lane 4*) in a manner that was more than additive of the effects of either protein alone. These results suggest that Ubc9 contributes to MR-dependent transcriptional activation at least partly by binding SRC-1 and recruiting it to cellular transcriptional machinery. Because recent reports (56) showed that relatively few coactivators, including SRC-1, strongly interact with MR in the presence of aldosterone, these findings are consistent with our data that Ubc9 and SRC-1 cooperatively function as coactivators of MR.

Next, to prove that an MR-Ubc9-SRC-1 complex contributes to MR-dependent transactivation in cells, we examined the physical association between MR, Ubc9, and SRC-1 using coimmunoprecipitation assays. First of all, endogenous Ubc9 was clearly associated with SRC-1 (Fig. 10*A*, *lane 1*), and the interaction was more pronounced when Ubc9 was ectopically overexpressed (Fig. 10*A*, *lane 2*). In addition, the N-terminal domain of MR-(1–670) was coimmunoprecipitated with SRC-1 (Fig. 10*B*, *top panel, lanes 3* and *4*), and the interaction was slightly enhanced when ectopic Ubc9 was overexpressed, which suggests Ubc9 may stabilize SRC-1 protein, thus increasing in MR-SRC-1 association as shown recently (57). Full-length MR was coimmunoprecipitated with Ubc9 as well as SRC-1 in the presence of aldosterone (data not shown). Taken together with these coimmunoprecipitation data, both Ubc9 and SRC-1 were shown to form a complex with the N-terminal domain of MR-(1–670), thus transactivating MR-dependent transcription.

*MR and Ubc9 Are Specifically Recruited to the MRE of Human ENaC Gene Promoter*—As mentioned above, the MR-Ubc9 complex activated the human *ENaC* gene transcription (Fig. 4*A*). ChIP assays were used to test whether stably expressing MR and endogenous Ubc9 are recruited to the endogenous *ENaC* gene promoter in 293-MR cells. The cross-linked, sheared chromatin preparations were subjected to immunoprecipitation with various antibodies, and the precipitated

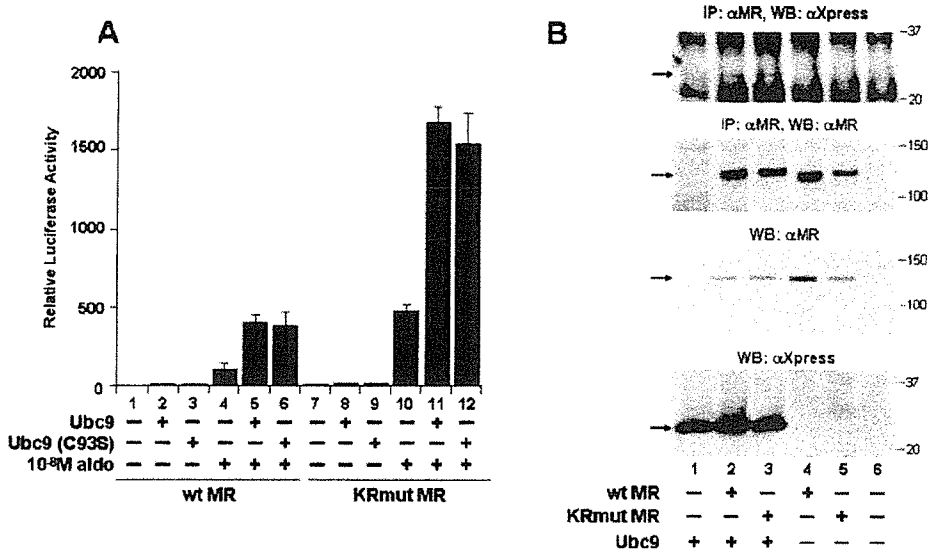


FIGURE 8. **Both Ubc9 and Ubc9 (C93S) enhance aldosterone-mediated transcription of wild type as well as K89R/K399R/K494R/K953R MR.** *A*, both Ubc9 and Ubc9(C93S) enhanced aldosterone-mediated transactivation of wild type- as well as KRmut-MR (K89R/K399R/K494R/K953R). HEK293 cells were transfected with 0.61 $\mu$g of total DNA, including 0.3 $\mu$g of *3xMRE-E1b-Luc* reporter, 0.1 $\mu$g of wild type (pRShMR) or K89R/K399R/K494R/K953R (pRShMR-KRmut), 0.2 $\mu$g of wild type Ubc9 or Ubc9 (C93S), and 0.01 $\mu$g of phRL-null. Twenty four hours post-transfection, cells were treated with vehicle or $10^{-8}$ M aldosterone. Cells were harvested at 48 h post-transfection and assayed for luciferase activity. Assays were performed in three separate experiments, each with triplicate samples. *B*, Ubc9 is associated with wild type as well as K89R/K399R/K494R/K953R MR in HEK293 cells. HEK293 cells were transfected with wild type (pRShMR) or KRmut MR (pRShMR-KRmut) and Xpress-tagged Ubc9 (pcDNA3.1/His-Ubc). Cells were harvested at 48 h after transfection. Whole cell extracts were immunoprecipitated (*IP*) with anti-MR antibody, and immunoprecipitates were subsequently analyzed by WB with anti-Xpress (*upper panel*) or anti-MR (*2nd panel*) antibody. Levels of proteins of MR and Ubc9 were determined by WB with anti-MR (*3rd panel*) and anti-Xpress (*bottom panel*) antibodies, respectively.

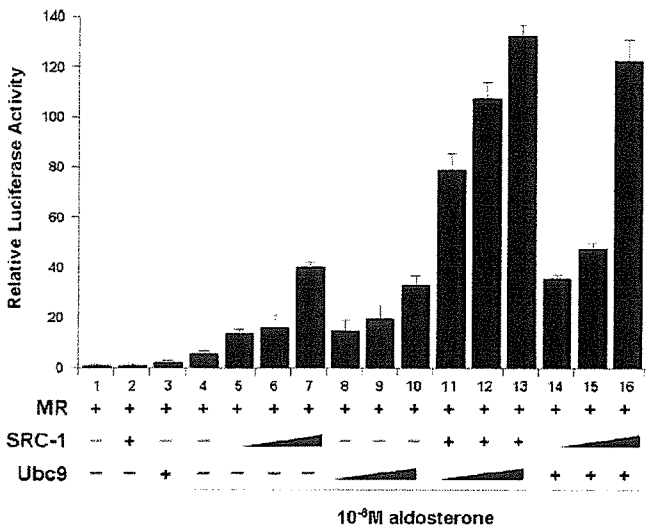


FIGURE 9. **Ubc9 and SRC-1 synergistically enhance MR-mediated transactivation.** Ubc9 and SRC-1 synergistically enhance aldosterone-mediated MR transactivation of *3xMRE-E1b-Luc* reporter in COS-1 cells. COS-1 cells were transfected with 0.81 $\mu$g of total DNA, including 0.1 $\mu$g of MR (pRShMR), 0.03, 0.1, or 0.2 $\mu$g of SRC-1 (pCR3.1-hSRC-1), 0.03, 0.1, or 0.2 $\mu$g of Ubc9 constructs (pcDNA3.1/His-Ubc9), 0.01 $\mu$g of phRL-null with 0.3 $\mu$g *3xMRE-E1b*-luciferase (*3xMRE-E1b-Luc*) reporter DNA for each well of the 24-well dish indicated. Twenty hour hours post-transfection, cells were treated with vehicle or $10^{-8}$ M aldosterone and harvested at 48 h post-transfection. The cell extracts were then assayed for luciferase activity. Assays were performed in three separate experiments, each with triplicate samples.

DNA was analyzed by PCR amplification of the MRE (−1567/−1297) of the *ENaC* promoter. We have confirmed the size of the sonicated DNA was ~300−600 bp, and these bands looked uniform (data not shown). When aldosterone is present in 293-MR cells, antibodies against MR, SRC-1, and Ubc9 efficiently immunoprecipitated the MRE (−1567/−1297) of the *ENaC* promoter only in the presence of aldosterone but not in the absence (Fig. 11). Normal IgG and no antibody (data not shown) failed to precipitate the *ENaC* promoter. In contrast to the MRE of the *ENaC* promoter, the control region (+1/+265) of the *ENaC* gene was not detected in association with MR or Ubc9 (Fig. 11). These data highlight a finding that endogenous MR and Ubc9 are recruited to an aldosterone-sensitive gene promoter in a largely hormone-dependent manner in the context of chromatin *in vivo*.

*Colocalization of MR with Ubc9 and SRC-1 in Cultured HEK293 Cells and the Collecting Duct Cells from Mouse Kidney*—To determine whether MR, Ubc9, and SRC-1 could interact within a cellular environment, HEK293 cells were transfected with DsRed-tagged MR, EGFP-tagged Ubc9, YFP-tagged SRC-1, alone or in various combinations, and photographed using fluorescence microscopy (Fig. 12, *A* and *B*). After cotransfection of HEK293 cells with pEGFP-Ubc9 and pDsRed-MR, EGFP-Ubc9 was localized in both nucleus and cytoplasm, whereas DsRed-MR was mainly localized in the cytoplasm in the presence of ethanol (vehicle). Treatment with $10^{-8}$ M aldosterone resulted in nuclear accumulation of DsRed-MR, which was overlapped with EGFP-Ubc9 (Fig. 12*A*). Similarly, after cotransfection of HEK293 cells with YFP-SRC-1 and DsRed-MR, YFP-SRC-1 was localized in the nucleus and cytoplasm, whereas DsRed-MR was mainly localized in the cytoplasm in the presence of ethanol (vehicle). Treatment with $10^{-8}$ M aldosterone resulted in nuclear accumulation of DsRed-MR and YFP-SRC-1 with occasional dot formation. These findings indicate that MR was colocalized with Ubc9 and SRC-1 in the nuclei only in the presence of aldosterone. The fluorescence imagings of ectopic expressing MR, Ubc9, and SRC-1 support colocalization of these proteins in cultured cells.

Finally, to examine whether the physical interaction between MR, Ubc9, and SRC-1 had a potentially physiological significance, we investigated whether endogenous MR, Ubc9, and SRC-1 were indeed colocalized within the mouse kidney as an aldosterone-sensitive tissue by immunohistochemical analysis (Fig. 13, *A* and *B*). As shown in Fig. 13, *A* and *B*, using specific

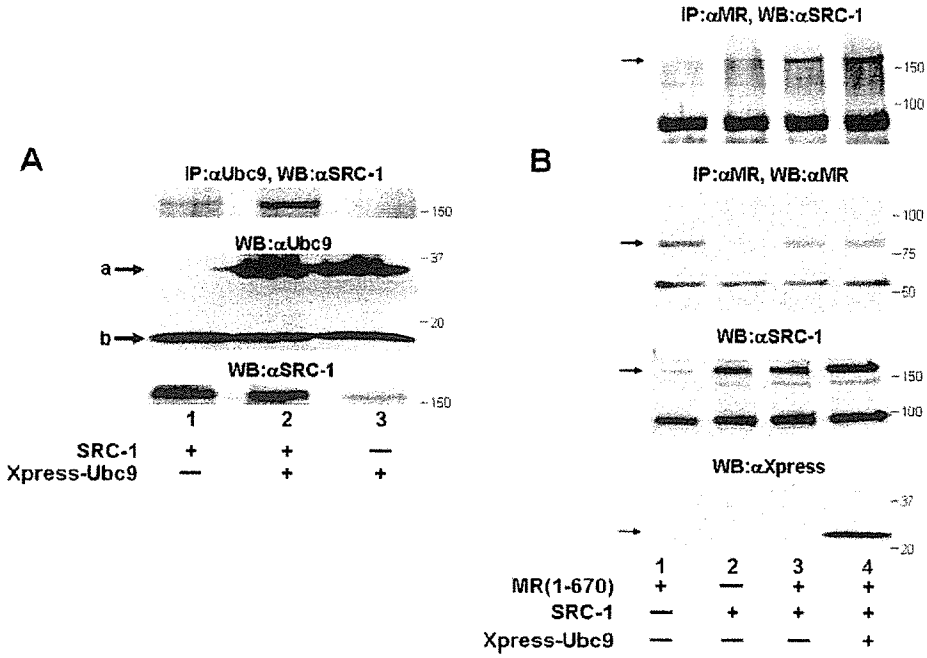


FIGURE 10. **Ubc9, SRC-1, and the N-terminal MR-(1–670) form a ternary complex *in vivo*.** *A*, Ubc9 was coimmunoprecipitated with SRC-1 in HEK293 cells. HEK293 cells were transfected with a combination of SRC-1 and Xpress-tagged Ubc9. Forty eight hours post-transfection, cells were harvested. Whole cell extracts were immunoprecipitated (*IP*) with anti-Ubc9 antibody, followed by immunoblotting with anti-SRC-1 antibody. Expression of Ubc9 and SRC-1 was also shown in WB with anti-Ubc9 and anti-SRC-1 antibodies, respectively. In the Western blotting with anti-Ubc9 antibody (*middle panel*), slower migrating bands (*a*) correspond to Xpress-tagged Ubc9, and faster migrating ones correspond to endogenous Ubc9 (*b*). *B*, SRC-1 was coimmunoprecipitated with the N-terminal MR-(1–670) in HEK293 cells. HEK293 cells were transfected with combination of N-terminal MR-(1–670), SRC-1, and Xpress-tagged Ubc9. Forty eight hours post-transfection, cells were harvested. Whole cell extracts were immunoprecipitated with anti-MR antibody, and immunoprecipitates were subsequently analyzed by WB with anti-SRC-1 and anti-MR antibody. Expression of SRC-1 and Ubc9 was also shown in WB with anti-SRC-1 and anti-Xpress antibodies. Ectopic expression of Ubc9 apparently pronounced interaction between MR-(1–670) and SRC-1.

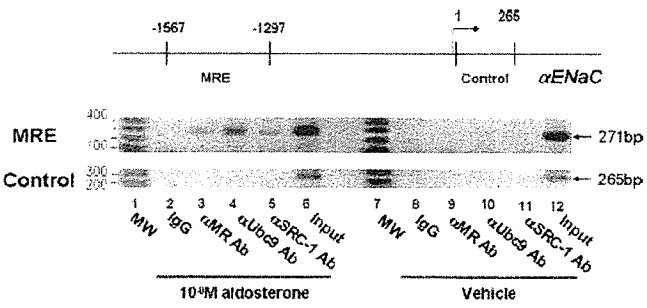


FIGURE 11. **MR and Ubc9 are recruited to the native *αENaC* promoter in an aldosterone-dependent manner.** For ChIP assays, when in the presence and absence (vehicle) of $10^{-8}$ M aldosterone, sheared chromatin from 293-MR cells was immunoprecipitated with anti-MR, anti-Ubc9, anti-SRC-1, or normal IgG. The coprecipitated DNA was amplified by PCR, using primers to amplify the *ENaC* promoter containing MRE or control region. MR and Ubc9 interact with −1567/−1297 DNA segment containing MRE but not with the 1/265 region of the *ENaC* gene (*Control*) in 293-MR cells. Immunoprecipitation with normal IgG (*lanes 2* and *8*) was used as negative controls.

antibodies, we were able to demonstrate that MR interacted with Ubc9 as well as SRC-1 in the nuclei of cortical collecting duct cells of mouse kidney. The results from cell-based reporter assays, coimmunoprecipitation, ChIP, fluorescence imagings, and immunohistochemistry strongly support a physiological role of Ubc9 in MR transactivation in cooperation with SRC-1 *in vivo*.

## DISCUSSION

In this study, we describe Ubc9, which interacts with the N-terminal transactivation domain of MR. Transient transfection assays together with small interfering RNA and RT-PCR indicated a physiological role of Ubc9 as a coactivator for the MR-dependent transactivation. Furthermore, the coimmunoprecipitation and ChIP assays clearly showed that endogenous Ubc9, SRC-1, and MR form a ternary complex. Colocalization of these proteins was also observed in the nuclei of intact mouse tissues, indicating that our observation is relevant to physiological events.

MR is modified by SUMO-1 via three consecutive enzyme reactions, including E2 enzyme Ubc9, thus resulting in transcriptional repression based on the fact that KRmut MR, which is a sumoylation-inactive mutant, disclosed enhanced aldosterone-mediated transactivation compared with wild type MR. Furthermore, desumoylation by overexpression of SENP1, a SUMO-1 isopeptidase, similarly potentiated MR-mediated transactivation (data not shown). These data indicate that sumoylation of MR leads to transcriptional repression. In fact, SUMO E3-ligase, PIAS1, was recently shown to function as a transcriptional corepressor of MR, the function of which is partly mediated by sumoylation of MR (38). The correlation between sumoylation and transcriptional repression is similarly shown in various nuclear receptors, such as glucocorticoid receptor (26–30) and androgen receptor (21, 22, 31, 32, 34–36, 58). Although sumoylation of MR results in transcriptional repression, this study shows a remarkable aspect of Ubc9 as a transcriptional coactivator for MR-mediated transactivation through formation of a complex with MR and SRC-1.

*Ubc9 Functions as a Transcriptional Coactivator of MR*—Ubc9 meets all the criteria for a transcriptional coactivator protein in the modulation of MR transcriptional properties. First, Ubc9 specifically interacted with MR in *in vitro* GST pulldown, yeast, and mammalian cells as shown in Figs. 1–3, and the interaction increased in the presence of aldosterone (Fig. 1). In addition, the interaction between the endogenous proteins was confirmed in 293-MR cells. All assays clearly showed that Ubc9 mainly interacted with the N-terminal MR-(1–670) containing AF-1 and DNA-binding domain but not with the C-terminal MR-(671–984) encompassing ligand-binding domain. Second, overexpression of Ubc9 had no effect on the reporter activities in the absence of transfected MR (Fig. 4*A*). However, Ubc9

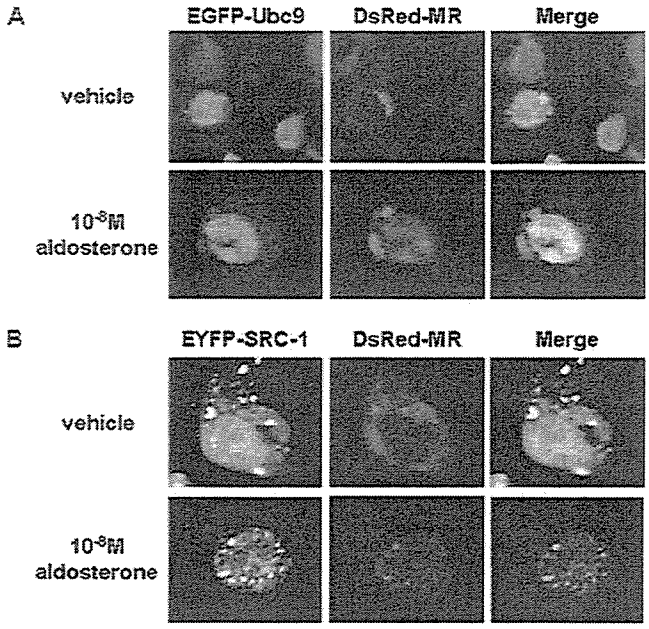


FIGURE 12. **Subcellular localization of MR, Ubc9, and SRC-1 in cultured HEK293 cells.** EGFP-Ubc9 (*A*) or YFP-SRC-1 (*B*) was cotransfected with DsRed-MR in the presence of ethanol (vehicle) and $10^{-8}$ M aldosterone in HEK293 cells. Both Ubc9 and SRC-1 were colocalized with MR in the presence of aldosterone in the nuclei of the transfected HEK293 cells.

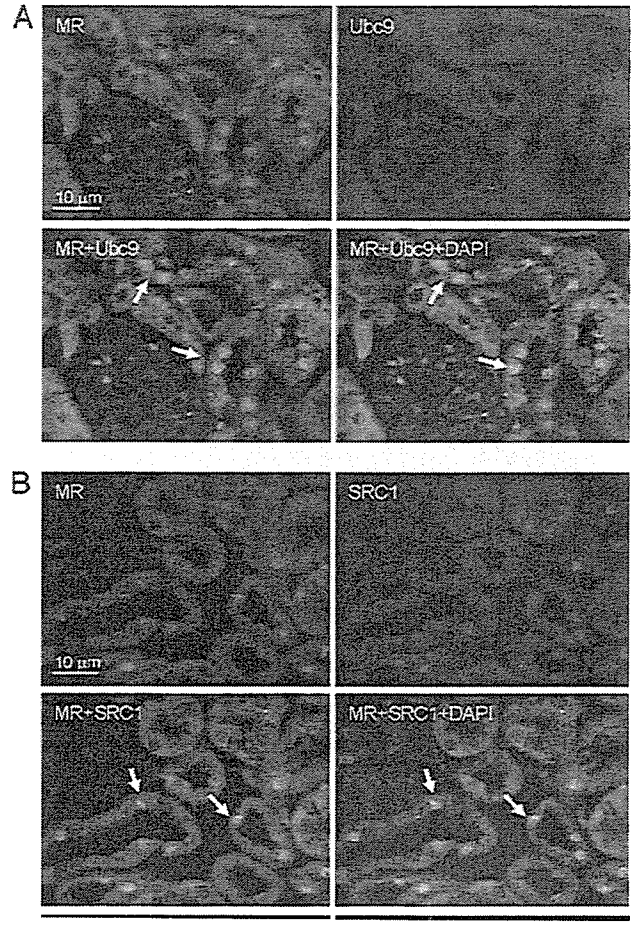


FIGURE 13. **Colocalization of MR with Ubc9 (*A*) and SRC-1 (*B*) in the nuclei of the collecting duct cells from mouse kidney.** Mouse kidney was used to immunologically detect Ubc9, SRC-1, and MR. MR was colocalized with Ubc9 (*A*) as well as SRC-1 (*B*) in the nuclei of collecting duct cells but not glomerulus or mesangial cells. *Arrows* indicate representative nuclear colocalization of MR and Ubc9 or SRC-1. Panels of MR were incubated with mouse anti-MR antibody, followed by Alexa Fluor 488-conjugated anti-mouse IgG, whereas panels of SRC-1 and Ubc9 were incubated with rabbit anti-SRC-1 and anti-Ubc9, respectively, followed by Alexa Fluor 594-conjugated anti-rabbit IgG. Panels of MR + Ubc9 or MR + SRC-1 were merged by each image. Nuclear staining was performed by 4′,6-diamino-2-phenylindole (*DAPI*). *Scale bar*, 10 μm.

potentiated the transactivation of three reporter constructs mediated by MR. Third, reduction of endogenous Ubc9 by small interfering RNA decreased MR-mediated transactivation of the reporter construct as well as an endogenous *Sgk* gene, indicating that endogenous Ubc9 normally contributes to MR-mediated transactivation. Fourth, ChIP assays clearly showed that endogenous MR and Ubc9 were recruited to a native MR-regulated *ENaC* promoter, demonstrating functional coupling between MR and Ubc9. Therefore, Ubc9 possesses all the characteristics expected for the transcriptional coactivator protein of MR.

To confirm further that Ubc9 is a coactivator of MR, we ruled out several possible ways in which the protein might enhance MR-mediated transactivation. First, as SUMO-1 conjugation plays an important role in protein modification, the effect of Ubc9 on MR transactivation might be the result of effects of Ubc9 on MR protein concentrations. Our preliminary experiments showed that overexpression of Ubc9 did not alter MR protein concentration in HEK293 cells (Fig. 3*B*). Second, it is also possible that overexpression of Ubc9 increases the concentrations of some coactivators or decreases the concentrations of some corepressors, which have been shown to interact with MR, but our preliminary results showed that overexpression of Ubc9 did not alter the protein concentration of SRC-1, GRIP1, or SMRT in the cells (data not shown). Because these experiments were performed by transient transfection, we are not able to conclude unequivocally that Ubc9 has no effects on the coregulator concentration, and further investigation is required. Third, another possibility is that overexpression of Ubc9 increases the DNA-binding affinity of MR. To exclude this possibility, we performed electrophoretic mobility shift assays to determine whether *in vitro* transcription-translated Ubc9 or extracts from cells overexpressing Ubc9 proteins affect the binding of MR to its response element DNA. The results showed that Ubc9 has no effect on MR binding to the response element (data not shown). Fourth, it has been proposed that SUMO-1 conjugation targets proteins to different cellular localizations. SF-1 can be directed into nuclear speckles and sequestered from the nucleolus in the presence of SUMO-1, thus resulting in transcriptional repression (43). It is therefore important to investigate whether and how MR activity and subcellular localization are functionally linked for further investigation. From these findings, Ubc9 clearly functions as a coactivator of MR *in vivo*.

Our data showed that both wild type and a sumoylation-inactive mutant of Ubc9 (C93S) similarly enhanced a reporter activity mediated by MR, indicating that coactivation of MR-mediated transcription by Ubc9 is likely to be independent of sumoylation activity. However, it is possible that ectopically produced Ubc9 regulate MR-mediated transactivation through

not only sumoylation of MR but also conjugation of SUMO-1 to one or more other cellular factors involved in transcriptional regulation.

*MR-Ubc9-SRC-1 Complexes Are Crucial for MR Transactivation*—Although our data showed that Ubc9 interacted with the N-terminal but not with the ligand-binding domain of MR, Ubc9 functions as a strict ligand-dependent coactivator of MR. We therefore presumed that Ubc9 should be indirectly associated with the ligand-binding domain of MR through certain coactivator(s). We then found the combined effects of Ubc9 and SRC-1, but not GRIP-1, p/CIP, or CBP/p300 on MR-dependent transactivation in transient transfection assays. Indeed, on aldosterone treatment, MR, Ubc9, and SRC-1 were recruited to an MR-responsive gene promoter in ChIP assays, indicating that these three proteins may form a complex. Because Ubc9 does not contain an autonomous activation domain when fused to the Gal4 DNA-binding domain, it seems likely that Ubc9 supports the transactivating effects of SRC-1 by acting as a scaffolding protein that stabilizes SRC-1 within the MR transcriptional complex or by stabilizing the SRC-1 protein level as shown recently (57). We showed that both Ubc9 and SRC-1 interacted with the N-terminal MR-(1–670) containing AF-1 domain. Ubc9 is also associated with SRC-1 (Fig. 10). A recent report (59) showed that SRC-1 is sumoylated, thus resulting in enhancing coactivation capacities for steroid receptors. Taken together with Fig. 10 and Ref. 59, it is likely that Ubc9 directly interacts with SRC-1. These results may provide a structural framework for the formation of a complex of these three proteins. Furthermore, fluorescence imagings and immunohistochemical analysis supported that MR was colocalized with Ubc9 and SRC-1 in the nuclei of cultured HEK293 cells and the collecting duct cells from mouse kidney, supporting the function of these complexes *in vivo*.

These results clearly showed that Ubc9 may have dual functions on MR. One function is sumoylation of MR through SUMO E2-conjugating enzyme activity, thus resulting in attenuation of ligand-dependent MR transactivation as shown previously (38). Another one is a new function as an MR coactivator by formation of a complex with SRC-1 and N-terminal MR beyond the SUMO E2-conjugating enzyme. Spatiotemporal regulation of these dual functions remains to be clarified.

*Acknowledgments—We thank Dr. Bert W. O'Malley, Dr. Ronald M. Evans, Dr. Ronald T. Hay, Dr. Jorma Palvimo, Dr. Christie P. Thomas, and Dr. Toshihiko Yanase for plasmid contributions.*

REFERENCES


1. Arriza, J. L., Weinberger, C., Cerelli, G., Glaser, T. M., Handelin, B. L., Housman, D. E., and Evans, R. M. (1987) *Science* **237,** 268–275
2. Le Menuet, D., Viengchareun, S., Muffat-Joly, M., Zennaro, M. C., and Lombes, M. (2004) *Mol. Cell. Endocrinol.* **217,** 127–136
3. Funder, J. W. (2003) *Exp. Opin. Investig. Drugs* **12,** 1963–1969
4. Fiebeler, A., and Haller, H. (2003) *Nephron. Physiol.* **94,** 47–50
5. Pitt, B., Zannad, F., Remme, W. J., Cody, R., Castaigne, A., Perez, A., Palensky, J., and Wittes, J. (1999) *N. Engl. J. Med.* **341,** 709–717
6. Pitt, B., Remme, W., Zannad, F., Neaton, J., Martinez, F., Roniker, B., Bittman, R., Hurley, S., Kleiman, J., and Gatlin, M. (2003) *N. Engl. J. Med.* **348,** 1309–1321
7. McKenna, N. J., and O'Malley, B. W. (2002) *Cell* **108,** 465–474
8. Shibata, H., Spencer, T. E., Onate, S. A., Jenster, G., Tsai, S. Y., Tsai, M. J., and O'Malley, B. W. (1997) *Recent Prog. Horm. Res.* **52,** 141–165
9. Smith, C. L., and O'Malley, B. W. (2004) *Endocr. Rev.* **25,** 45–71
10. Hermanson, O., Glass, C. K., and Rosenfeld, M. G. (2002) *Trends Endocrinol. Metab.* **13,** 55–60
11. Rosenfeld, M. G., and Glass, C. K. (2001) *J. Biol. Chem.* **276,** 36865–36868
12. Li, Y., Suino, K., Daugherty, J., and Xu, H. E. (2005) *Mol. Cell* **19,** 367–380
13. Onate, S. A., Tsai, S. Y., Tsai, M. J., and O'Malley, B. W. (1995) *Science* **270,** 1354–1357
14. Kamei, Y., Xu, L., Heinzel, T., Torchia, J., Kurokawa, R., Gloss, B., Lin, S. C., Heyman, R. A., Rose, D. W., Glass, C. K., and Rosenfeld, M. G. (1996) *Cell* **85,** 403–414
15. Johnson, E. S. (2004) *Annu. Rev. Biochem.* **73,** 355–382
16. Verger, A., Perdomo, J., and Crossley, M. (2003) *EMBO Rep.* **4,** 137–142
17. Gill, G. (2004) *Genes Dev.* **18,** 2046–2059
18. Seeler, J. S., and Dejean, A. (2003) *Nat. Rev. Mol. Cell Biol.* **4,** 690–699
19. Hay, R. T. (2005) *Mol. Cell* **18,** 1–12
20. Kahyo, T., Nishida, T., and Yasuda, H. (2001) *Mol. Cell* **8,** 713–718
21. Kotaja, N., Aittomaki, S., Silvennoinen, O., Palvimo, J. J., and Janne, O. A. (2000) *Mol. Endocrinol.* **14,** 1986–2000
22. Nishida, T., and Yasuda, H. (2002) *J. Biol. Chem.* **277,** 41311–41317
23. Kirsh, O., Seeler, J. S., Pichler, A., Gast, A., Muller, S., Miska, E., Mathieu, M., Harel-Bellan, A., Kouzarides, T., Melchior, F., and Dejean, A. (2002) *EMBO J.* **21,** 2682–2691
24. Pichler, A., Gast, A., Seeler, J. S., Dejean, A., and Melchior, F. (2002) *Cell* **108,** 109–120
25. Kagey, M. H., Melhuish, T. A., and Wotton, D. (2003) *Cell* **113,** 127–137
26. Cho, S., Kagan, B. L., Blackford, J. A., Jr., Szapary, D., and Simons, S. S., Jr. (2005) *Mol. Endocrinol.* **19,** 290–311
27. Gottlicher, M., Heck, S., Doucas, V., Wade, E., Kullmann, M., Cato, A. C., Evans, R. M., and Herrlich, P. (1996) *Steroids* **61,** 257–262
28. Kaul, S., Blackford, J. A., Jr., Cho, S., and Simons, S. S., Jr. (2002) *J. Biol. Chem.* **277,** 12541–12549
29. Le Drean, Y., Mincheneau, N., Le Goff, P., and Michel, D. (2002) *Endocrinology* **143,** 3482–3489
30. Tian, S., Poukka, H., Palvimo, J. J., and Janne, O. A. (2002) *Biochem. J.* **367,** 907–911
31. Gross, M., Yang, R., Top, I., Gasper, C., and Shuai, K. (2004) *Oncogene* **23,** 3059–3066
32. Kotaja, N., Karvonen, U., Janne, O. A., and Palvimo, J. J. (2002) *Mol. Cell. Biol.* **22,** 5222–5234
33. Kotaja, N., Karvonen, U., Janne, O. A., and Palvimo, J. J. (2002) *J. Biol. Chem.* **277,** 30283–30288
34. Poukka, H., Aarnisalo, P., Karvonen, U., Palvimo, J. J., and Janne, O. A. (1999) *J. Biol. Chem.* **274,** 19441–19446
35. Poukka, H., Karvonen, U., Janne, O. A., and Palvimo, J. J. (2000) *Proc. Natl. Acad. Sci. U. S. A.* **97,** 14145–14150
36. Tan, J., Hall, S. H., Hamil, K. G., Grossman, G., Petrusz, P., Liao, J., Shuai, K., and French, F. S. (2000) *Mol. Endocrinol.* **14,** 14–26
37. Abdel-Hafiz, H., Takimoto, G. S., Tung, L., and Horwitz, K. B. (2002) *J. Biol. Chem.* **277,** 33950–33956
38. Tallec, L. P., Kirsh, O., Lecomte, M. C., Viengchareun, S., Zennaro, M. C., Dejean, A., and Lombes, M. (2003) *Mol. Endocrinol.* **17,** 2529–2542
39. Sentis, S., Le Romancer, M., Bianchin, C., Rostan, M. C., and Corbo, L. (2005) *Mol. Endocrinol.* **19,** 2671–2684
40. Floyd, Z. E., and Stephens, J. M. (2004) *Obes. Res.* **12,** 921–928
41. Ohshima, T., Koga, H., and Shimotohno, K. (2004) *J. Biol. Chem.* **279,** 29551–29557
42. Yamashita, D., Yamaguchi, T., Shimizu, M., Nakata, N., Hirose, F., and Osumi, T. (2004) *Genes Cells* **9,** 1017–1029
43. Chen, W. Y., Lee, W. C., Hsu, N. C., Huang, F., and Chung, B. C. (2004) *J. Biol. Chem.* **279,** 38730–38735
44. Komatsu, T., Mizusaki, H., Mukai, T., Ogawa, H., Baba, D., Shirakawa, M., Hatakeyama, S., Nakayama, K. I., Yamamoto, H., Kikuchi, A., and Morohashi, K. (2004) *Mol. Endocrinol.* **18,** 2451–2462
45. Lee, M. B., Lebedeva, L. A., Suzawa, M., Wadekar, S. A., Desclozeaux, M., and Ingraham, H. A. (2005) *Mol. Cell. Biol.* **25,** 1879–1890
46. Kitagawa, H., Fujiki, R., Yoshimura, K., Mezaki, Y., Uematsu, Y., Matsui,

D., Ogawa, S., Unno, K., Okubo, M., Tokita, A., Nakagawa, T., Ito, T., Ishimi, Y., Nagasawa, H., Matsumoto, T., Yanagisawa, J., and Kato, S. (2003) *Cell* **113,** 905–917
47. Watanabe, M., Yanagisawa, J., Kitagawa, H., Takeyama, K., Ogawa, S., Arao, Y., Suzawa, M., Kobayashi, Y., Yano, T., Yoshikawa, H., Masuhiro, Y., and Kato, S. (2001) *EMBO J.* **20,** 1341–1352
48. Yanagisawa, J., Kitagawa, H., Yanagida, M., Wada, O., Ogawa, S., Nakagomi, M., Oishi, H., Yamamoto, Y., Nagasawa, H., McMahon, S. B., Cole, M. D., Tora, L., Takahashi, N., and Kato, S. (2002) *Mol. Cell* **9,** 553–562
49. Kobayashi, S., Shibata, H., Kurihara, I., Yokota, K., Suda, N., Saito, I., and Saruta, T. (2004) *J. Mol. Endocrinol.* **32,** 69–86
50. Kurihara, I., Shibata, H., Kobayashi, S., Suda, N., Ikeda, Y., Yokota, K., Murai, A., Saito, I., Rainey, W. E., and Saruta, T. (2005) *J. Biol. Chem.* **280,** 6721–6730
51. Mick, V. E., Itani, O. A., Loftus, R. W., Husted, R. F., Schmidt, T. J., and Thomas, C. P. (2001) *Mol. Endocrinol.* **15,** 575–588
52. Shibata, H., Nawaz, Z., Tsai, S. Y., O'Malley, B. W., and Tsai, M. J. (1997) *Mol. Endocrinol.* **11,** 714–724
53. Kobayashi, S., Shibata, H., Yokota, K., Suda, N., Murai, A., Kurihara, I., Saito, I., and Saruta, T. (2004) *Endocr. Res.* **30,** 617–621
54. Saitoh, M., Takayanagi, R., Goto, K., Fukamizu, A., Tomura, A., Yanase, T., and Nawata, H. (2002) *Mol. Endocrinol.* **16,** 694–706
55. Iniguez-Lluhi, J. A., and Pearce, D. (2000) *Mol. Cell. Biol.* **20,** 6040–6050
56. Hultman, M. L., Krasnoperova, N. V., Li, S., Du, S., Xia, C., Dietz, J. D., Lala, D. S., Welsch, D. J., and Hu, X. (2005) *Mol. Endocrinol.* **19,** 1460–1473
57. Lu, Z., Wu, H., and Mo, Y. Y. (2006) *Exp. Cell Res.* **312,** 1865–1875
58. Kotaja, N., Vihinen, M., Palvimo, J. J., and Janne, O. A. (2002) *J. Biol. Chem.* **277,** 17781–17788
59. Chauchereau, A., Amazit, L., Quesne, M., Guiochon-Mantel, A., and Milgrom, E. (2003) *J. Biol. Chem.* **278,** 12335–12343

# Novel axonal projection from the caudal end of the ventrolateral medulla to the intermediolateral cell column

**Kamon Iigaya, Hiroo Kumagai, Hiroshi Onimaru, Akira Kawai, Naoki Oshima, Toshiko Onami, Chie Takimoto, Tadashi Kamayachi, Koichi Hayashi, Takao Saruta and Hiroshi Itoh**

*Am J Physiol Regulatory Integrative Comp Physiol* 292:927-936, 2007. First published Nov 2, 2006; doi:10.1152/ajpregu.00254.2006



***The American Journal of Physiology - Regulatory, Integrative and Comparative Physiology*** publishes original investigations that illuminate normal or abnormal regulation and integration of physiological mechanisms at all levels of biological organization, ranging from molecules to humans, including clinical investigations. It is published 12 times a year (monthly) by the American Physiological Society, 9650 Rockville Pike, Bethesda MD 20814-3991. Copyright © 2005 by the American Physiological Society. ISSN: 0363-6119, ESSN: 1522-1490. Visit our website at http://www.the-aps.org/.

*Am J Physiol Regul Integr Comp Physiol* 292: R927–R936, 2007.
First published November 2, 2006; doi:10.1152/ajpregu.00254.2006.

# Novel axonal projection from the caudal end of the ventrolateral medulla to the intermediolateral cell column

**Kamon Iigaya,[1] Hiroo Kumagai,[1] Hiroshi Onimaru,[2] Akira Kawai,[2] Naoki Oshima,[1] Toshiko Onami,[1] Chie Takimoto,[1] Tadashi Kamayachi,[1] Koichi Hayashi,[1] Takao Saruta,[1] and Hiroshi Itoh[1]**

[1]*Department of Internal Medicine, Keio University School of Medicine and*
[2]*Department of Physiology, Showa University School of Medicine, Tokyo, Japan*

Submitted 13 April 2006; accepted in final form 30 September 2006

**Kamon I, Kumagai H, Onimaru H, Kawai A, Oshima N, Onami T, Takimoto C, Kamayachi T, Hayashi K, Saruta T, Itoh H.** Novel axonal projection from the caudal end of the ventrolateral medulla to the intermediolateral cell column. *Am J Physiol Regul Integr Comp Physiol* 292: R927–R936, 2007. First published November 2, 2006; doi:10.1152/ajpregu.00254.2006.—We used an optical imaging technique to investigate whether axons of neurons in the caudal end of the ventrolateral medulla (CeVLM), as well as axons of neurons in the rostral ventrolateral medulla (RVLM), project to neurons in the intermediolateral cell column (IML) of the spinal cord. Brain stem-spinal cord preparations from neonatal normotensive Wistar-Kyoto and spontaneously hypertensive rats were stained with a voltage-sensitive dye, and responses to electrical stimulation of the IML at the $Th_2$ level were detected as changes in fluorescence intensity with an optical imaging apparatus (MiCAM-01). The results were as follows: *1*) depolarizing responses to IML stimulation during low-Ca high-Mg superfusion were detected on the ventral surface of the medulla at the level of the CeVLM, as well as at the level of the RVLM, *2*) depolarizing responses were also detected on cross sections at the level of the CeVLM, and they had a latency of 24.0 ± 5.5 (SD) ms, *3*) antidromic action potentials in response to IML stimulation were demonstrated in the CeVLM neurons where optical images were detected, and *4*) glutamate application to the CeVLM increased the frequency of excitatory postsynaptic potentials (EPSPs) and induced depolarization of the IML neurons. The optical imaging findings suggested a novel axonal and functional projection from neurons in the CeVLM to the IML. The increase in EPSPs of the IML neurons in response to glutamate application suggests that the CeVLM participates in the regulation of sympathetic nerve activity and blood pressure and may correspond to the caudal pressor area.

optical imaging; patch-clamp technique; monosynaptic bulbospinal projection; caudal pressor area; sympathetic nervous system

BECAUSE NEURONS IN THE intermediolateral cell column (IML) of the spinal cord receive various inputs from higher neurons [the rostral ventrolateral medulla (RVLM), rostral ventromedial medulla (RVMM), paraventricular nucleus, raphe nucleus, etc. (1, 4, 12, 21, 23, 26, 29)], IML neurons play an important role in the regulation of sympathetic outflow. The precise location and function of the caudal pressor area (CPA) have recently been reevaluated, and it is now known to be located more caudally than the caudal ventrolateral medulla (CVLM) (see Refs. 2, 8, 27, 28). Because microinjection of glutamate and homocysteine in the CPA in in vivo experiments induced sympathetic activation and an increase in blood pressure, and microinjection of glycine induced inhibition of sympathetic activity and blood pressure reduction, the neurons in the CPA have been considered to be sympathoexcitatory (16).

Much attention has been focused on afferent inputs in the CPA and efferent pathways out of the CPA. Natarajan and Morrison (16) demonstrated that the CPA neurons project to the sympathoexcitatory CVLM, whose neurons then project to the RVLM. Horiuchi et al. (8) reported that the CPA is modulated by prolactin-releasing peptide, a hypothalamic hormone. Sun and Panneton (27, 28) used anterograde and retrograde tracers to precisely localize the site of the CPA in the ventrolateral medulla (VLM). Li et al. (11) recently found a direct projection from the CPA to the IML in a retrograde tracer experiment. Studies to investigate whether the CPA neurons are anatomically and functionally bulbospinal neurons have just begun.

In the present study, we used optical imaging, electrophysiological, and histological methods to determine whether an axonal projection exists from the medulla oblongata, including the CPA, to the IML. Because we did not measure blood pressure in this in vitro study, we will refer to the area as the caudal end of the VLM (CeVLM), instead of as the CPA. Using optical imaging, we tried to detect depolarizing responses on the ventral surface of the medulla oblongata and cross sections of brain stem-spinal cord preparations to electrical stimulation of the axons or neural terminals of presympathetic neurons that projected to the IML region (IML stimulation). We also examined antidromic action potentials in response to the IML stimulation in the CeVLM area, in which optical imaging showed depolarizing responses. The preliminary results have been presented in the form of an abstract (9).

## MATERIALS AND METHODS

*Preparations and staining.* Experiments were performed on brain stem-spinal cord preparations from 2- to 4-day-old Wistar-Kyoto (WKY) rats and spontaneously hypertensive rats (SHRs) (see Refs. 14, 15, and 21). The experimental protocols were approved by the Animal Research Committee of Keio University School of Medicine in compliance with Japanese Law (no. 105). Under deep ether anesthesia, the brain stem and spinal cord were isolated as previously described (14), and the spinal cord was sectioned at the second thoracic nerve root ($Th_2$) level (Fig. 1). The following three different types of preparations were used: *1*) a type in which the brain stem was sectioned at the distal end of the pons for observation of the ventral surface of the medulla oblongata, *2*) a type in which the brain stem was sectioned between the posterior inferior cerebellar artery and the top of the hypoglossal nerve roots for observation of cross sections at

Address for reprint requests and other correspondence: H. Kumagai, Dept. of Internal Medicine, Keio Univ. School of Medicine, 35 Shinanomachi, Shinjuku-ku, Tokyo 160-8582, Japan (e-mail: hkumagai@sc.itc.keio.ac.jp).

The costs of publication of this article were defrayed in part by the payment of page charges. The article must therefore be hereby marked "*advertisement*" in accordance with 18 U.S.C. Section 1734 solely to indicate this fact.

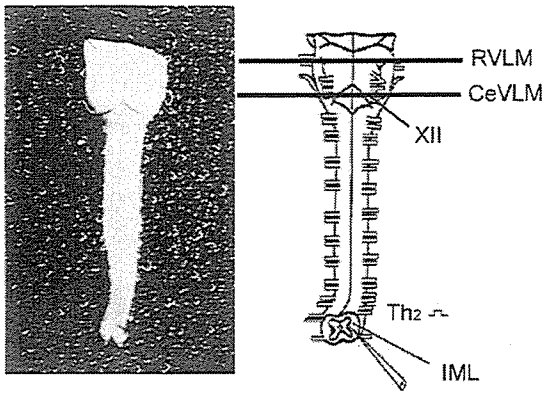


Fig. 1. Brain stem-spinal cord preparation from a neonatal spontaneously hypertensive rat. Three different types of preparations were used for optical imaging and the whole cell patch-clamp technique as follows: *1*) a type for observation on the ventral surface of the medulla oblongata, *2*) a type for observation of cross sections at the level of the rostral ventrolateral medulla (RVLM), and *3*) a type for observation of cross sections at the level of the caudal end of the VLM (CeVLM). Electrical stimulation was applied to the intermediolateral cell column (IML) at the $Th_2$ level.

the RVLM level, and *3*) a type in which the brain stem was sectioned between the branch point of the basilar artery and the distal end of the exit points of the hypoglossal nerve roots for observation of cross sections at the level of the CeVLM.

The preparations were continuously superfused at 2–3 ml/min with a standard solution, pH 7.4, consisting of (in mmol/l) 124 NaCl, 5.0 KCl, 2.4 $CaCl_2$, 1.3 $MgCl_2$, 26 $NaHCO_3$, 1.2 $KH_2PO_4$, and 30 D-glucose and equilibrated with 95% $O_2$ and 5% $CO_2$ at 26–27°C. In most of the experiments, the preparations were superfused with a low-Ca high-Mg solution containing (in mmol/l) 0.2 $CaCl_2$ and 5.0 $MgCl_2$ to exclude ascending monosynaptic and polysynaptic projections and descending polysynaptic projections and to detect descending monosynaptic projections alone.

*Optical imaging.* The brain stem-spinal cord preparations were incubated for 40–50 min in the standard solution containing the fluorescent voltage-sensitive dye Di-4-ANEPPS (0.1 mg/ml) or Di-2-ANEPEQ (50 μg/ml; Molecular Probes, Eugene, OR; see Refs. 19, 20, 30–32). The hydrophilic dye Di-2-ANEPEQ was used for observation at the brain stem surface because of its higher diffusion property into tissue than the lipophilic dye Di-4-ANEPPS. Di-4-ANEPPS was used for observation at the cut surface of the transverse sections because it provides more stable staining with less noise than Di-2-ANEPEQ. Previous study reported that the depth for optical detection of spontaneous bursting activity was <500 μm and that the effective depth might be 200–300 μm for Di-2-ANEPEQ (20). The depth for optical detection of responses to electrical stimulation may be greater than for spontaneous burst activity.

The preparation was then placed in a perfusion chamber (volume 1 ml) mounted on a fluorescence microscope (BX50WIF-2; Olympus Optical, Tokyo, Japan), with the ventral surface or cross section of the medulla and spinal cord facing up.

Neuronal activity in the preparation was detected as a change in fluorescence of the voltage-sensitive dye with an optical imaging apparatus (MiCAM01; Brain Vision, Tsukuba, Japan; see Refs. 19, 20, 31, 32) and a tungsten-halogen lamp (150 watts) through a 510–550-nm excitation filter, dichroic mirror, and 590-nm absorption filter (U-MWIG2 mirror unit; Olympus Optical). The head of charge-coupled device (CCD) camera had an 8.4 × 6.5 $mm^2$ imaging area consisting of 180 × 120 pixels and a maximal time resolution of 3.5 ms. The power of the microscope was adjusted to ×2 in most experiments, so that the image sensor could cover an area measuring 4.2 × 3.25 $mm^2$. We examined optical images of the medulla oblongata for responses to electrical stimulation of the IML. Very thin stainless steel electrodes (tip diameter 20 μm, length 100 μm, impedance 700 kΩ) were used, and the position of the IML neurons was carefully identified through the CCD camera to enable stimulation (10–50 volts, 100 μs, single pulse) of only axons that projected to the IML neurons as much as possible by inserting the electrode perpendicularly in cross sections of the spinal cord (Fig. 1). The IML was stimulated at the $Th_2$ level, which is known to be the main target region of the cardiac sympathetic premotor neurons in the brain stem.

Most recordings were performed with an acquisition time of 10 ms. Fluorescence signals during a 3.4-s period/trial were totaled and averaged for 10–20 electric stimulations of ipsilateral IML neurons. The fluorescence changes are expressed as ratios (fluorescence intensity divided by the fluorescence intensity of the reference image). The differential images were processed with a software-spatial filter for 2 × 2 pixels and presented as pseudocolor displays in which the "red" region corresponded to a decrease in fluorescence, meaning membrane depolarization. The intensity of the depolarizing response was strongest in the red region, grew weaker in the yellow region, and still weaker in the green region. Decreases in fluorescence (depolarization) are presented as upward of the intensity of the depolarization. Because optical signals basically represent depolarization of the soma and not of the axons (30), we refer to the fluorescence change as "a depolarizing response." Values are reported as means ± SD. Data were compared with assessment of statistical significance by the unpaired *t*-test.

*Electrophysiological experiments.* We investigated whether the neurons in the CeVLM that exhibited depolarizing responses to IML stimulation detected by optical imaging projected to the IML. Neuronal activity was recorded extracellularly or intracellularly during low-Ca high-Mg superfusion (21), and the IML was stimulated to investigate the induction of antidromic action potentials. For the extracellular recordings, glass electrodes were filled with 2% pontamine sky blue in 0.5 mol/l sodium acetate (resistance 5–20 MΩ). For the intracellular recordings by the whole cell patch-clamp technique, patch electrodes were filled with 0.5% lucifer yellow in a pipette solution of the following composition (mmol/l): 130 potassium gluconate, 10 EGTA, 10 HEPES, 2 $Na_2$-ATP, 1 $CaCl_2$, and 1 $MgCl_2$, with pH 7.2–7.3 adjusted with KOH. The IML was stimulated with a stainless steel electrode (5–15 volts, 100 μs, single pulse) to induce antidromic action potentials in the VLM.

In addition, to examine functional and orthodromic effects of CeVLM neurons on the IML, IML neurons were recorded by an intracellular technique (whole cell patch-clamp) and an extracellular technique during superfusion with standard solution. Glutamate (1 mmol/l, 10–30 μl) was locally applied to the CeVLM in a preparation whose cross section was at the level of the CeVLM and from which more rostral regions, including the CVLM and RVLM, have been removed (*type 3* preparation under *Preparations and staining* and Fig. 1). To confirm and minimize glutamate diffusion in the cross section at the level of the CeVLM, the glutamate solution was mixed with Fast Blue.

*Histological examination.* After immersing the preparations in 10% formalin-phosphate buffer solution at 4°C for 48 h, the medulla oblongata with spinal cord was cut into 100-μm sections, and the locations of neurons that had stained with lucifer yellow or pontamine sky blue were identified in the medulla and spinal cord. All preparations were then stained with neutral red to compare the location of the CeVLM neurons with the location of surrounding nuclei.

At the conclusion of the optical imaging experiments, the IML that had been electrically stimulated was coagulated (20 volts, 20 ms, single pulse) to confirm that the neurons that projected to the IML had been accurately stimulated.

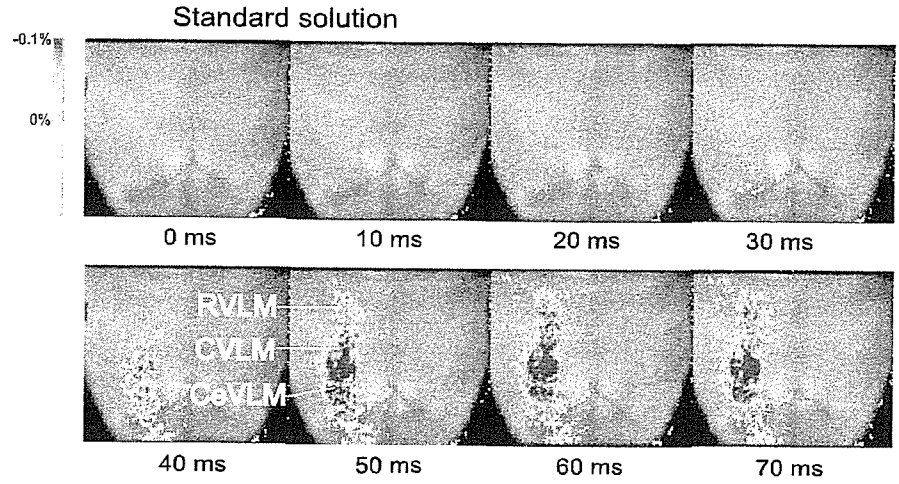


Fig. 2. Optical images of the ventral surface of the medulla oblongata during superfusion with standard solution. Depolarizing responses to IML stimulation were clearly detected on the ventral surface at the RVLM, the caudal ventrolateral medulla (CVLM), and the CeVLM ($n$ = 10).

To confirm that the neurons in the spinal cord that depolarized in response to glutamate application to the CeVLM were IML neurons, they were stained with lucifer yellow at the conclusion of the intracellular recording.

## RESULTS

*Optical imaging on the ventral surface.* Depolarizing responses were actually captured in the form of a motion picture. As shown in Fig. 2, during superfusion with standard solution, IML stimulation induced depolarizing responses on the continuous column of the surface of the rostrocaudal VLM, including the RVLM, the CVLM, and the CeVLM. In all preparations ($n$ = 10), the intensity of depolarization (fluorescence change) of the CeVLM (−0.098 ± 0.024%, means ± SD) was significantly ($P < 0.01$) stronger than that in the RVLM (−0.048 ± 0.024%) and CVLM. The latency between IML stimulation and the start and the peak of the depolarizing response at the CeVLM was 41 ± 15 and 82 ± 32 ms, respectively. No depolarizing responses were detected in other regions despite even stronger stimulation of the IML.

As shown in Fig. 3, the IML stimulation during low-Ca high-Mg superfusion also induced depolarizing responses on the surface of the rostrocaudal VLM, including the RVLM, the CVLM, and the CeVLM. The low-Ca high-Mg solution was used to exclude ascending monosynaptic and polysynaptic projections and descending polysynaptic projections and obtain only the depolarizing responses of descending monosynaptic projections. In all preparations ($n$ = 6), the depolarizing response of the CeVLM (−0.041 ± 0.009%) was significantly ($P < 0.05$) stronger than that of the RVLM (−0.026 ± 0.010%). The latency between IML stimulation and the start and the peak of depolarization in the CeVLM was 28 ± 7 and 31 ± 11 ms, respectively. The intensity of the depolarizing response was weaker during low-Ca high-Mg superfusion than during perfusion with the standard solution.

*Optical imaging of the cross sections.* IML stimulation during low-Ca high-Mg superfusion induced depolarizing responses in restricted regions on cross sections at the level of the RVLM ($n$ = 6; Fig. 4) and at the level of the CeVLM ($n$ = 8; Fig. 5). The latency between IML stimulation and the start and the peak of the depolarizing response was 24 ± 5 and 36 ± 8 ms, respectively, at the level of the CeVLM. That was 27 ± 9 and 35 ± 10 ms, respectively, at the level of the RVLM.

To determine whether the depolarizing responses were derived from the somas and not from the axons, we examined the depolarizing responses after adding γ-aminobutyric acid

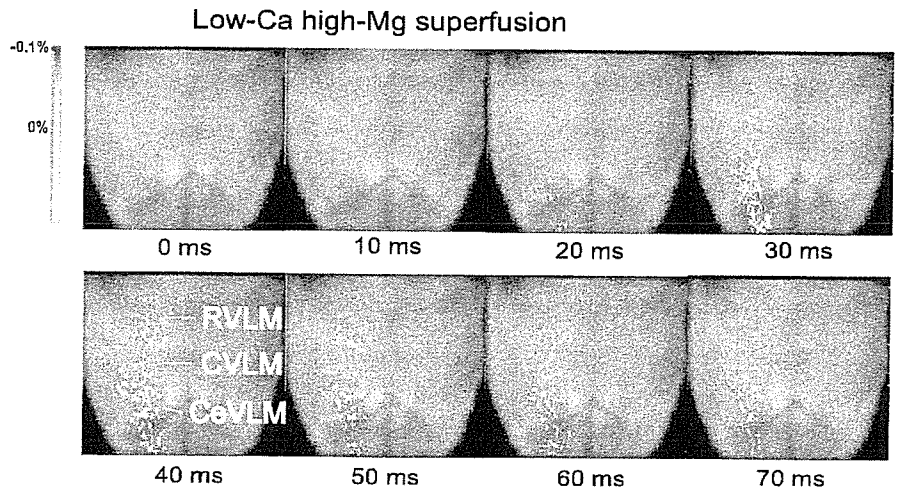


Fig. 3. Optical images of the ventral surface of the medulla oblongata during superfusion with low-Ca high-Mg solution. Depolarizing responses to IML stimulation were detected on the ventral surface at the RVLM, the CVLM, and the CeVLM ($n$ = 6).